Controlled grafting of multi-block copolymers for improving membrane properties for CO2 separation

Xavier Solimando, Jérôme Babin, Carole Arnal-Herault, Denis Roizard, Danielle Barth, Marc Ponçot, Isabelle Royaud, Pierre Alcouffe, Laurent David, Anne Jonquieres

Controlled grafting of multi-block copolymers for improving membrane properties for CO_2 separation

Xavier SOLIMANDO[1], Jérôme BABIN[1], Carole ARNAL-HERAULT[1], Denis ROIZARD[2], Danielle BARTH[2], Marc PONCOT[3], Isabelle ROYAUD[3], Pierre ALCOUFFE[4], Laurent DAVID[4], Anne JONQUIERES[1,*]

[1] Université de Lorraine, CNRS, LCPM, F-54000 Nancy, France

[2] Université de Lorraine, CNRS, LRGP, F-54000 Nancy, France

[3] Université de Lorraine, CNRS, IJL, F-54000 Nancy, France

[4] Laboratoire Ingénierie des Matériaux Polymères (IMP), Université Claude Bernard Lyon 1, Univ Lyon, CNRS UMR 5223, 15 Bd. André Latarjet, F-69622 Villeurbanne Cedex, France.

Keywords: poly(ethylene oxide); grafted multi-block copolymers; polyimides; CO_2-selective membranes

---

Abstract (202 words): Linear poly(ether-urea-imide)s (PUIs) are attractive multi-block segmented copolymers well-known for high selectivity for CO_2 separations. Their CO_2 permeability generally increases but their selectivity decreases with their polyether soft content limited to 70 wt% to preserve their mechanical properties. In this work, the grafting of a PUI copolymer with PEO-based soft grafts is reported for strongly increasing the membrane properties. The design of the grafted copolymers involved step-growth polymerization, controlled radical polymerization, and "click" chemistry. This strategy ensured the control of grafting rate, graft molecular weight and soft contents varying from 57 to 85 wt%. The membrane properties for CO_2 and N_2 permeation were correlated to the PUI chemical structure, morphology and soft content. The best membrane properties (P_{CO2} = 196 Barrer; $\alpha CO_2/N_2$ = 39 at 2 bar and 35°C) were obtained for PUI-g-1PEDEGA5000 corresponding to the highest grafting rate and graft length. Compared to the non-grafted PUI, the best grafted copolymer had much higher CO_2 permeability (×17) while the ideal separation factor $\alpha CO_2/N_2$ was maintained at high level, thus leading to separation properties very close to the Robeson 2008 upper-bound. By allowing very high contents of amorphous soft phase and specific morphology, the new grafting strategy offered high-performance membranes for CO_2 capture.

Corresponding author. Email address: anne.jonquieres@univ-lorraine.fr, tel: +33 3 72 74 37 05

1. Introduction

Carbon dioxide (CO_2) is the widely most produced greenhouse gas in the world from power plants [1,2], syngas production [3,4], natural gas extraction [5–7] and transport field [8]. CO_2 capture and storage are major challenges to limit its environmental effects and global warming [9,10]. Research in this area is very active, with implication of public and private partners, but the large-scale deployment of CO_2 capture and storage processes still requires significant research progress. Between many CO_2 capture strategies, such as cryogenic distillation, amine absorption or pressure swing adsorption, membrane separation appears as the most attractive process because of low energy consumption of only 70-75 kWh/ton of recovered CO_2 compared to 330-340 kWh/ton for the mostly used chemical absorption process using amine solvents [11]. Mechanisms of separation in these membranes are based on gas-polymer interactions (sorption) and mobility of gas through the free volume fraction of the material (diffusion).

Concerning the treatment of post-combustion gases, CO_2/N_2 is the most widely investigated separation in the literature. According to several reviews [12–20], the most efficient membranes for CO_2 separation are high porosity membranes, as polymers of intrinsic microporosity (PIMs) or thermally rearranged polymers (TRPs), ionic liquids-based and poly(ethylene oxide) (PEO)-based materials and related polymer blends and mixed matrix membranes. In particular, the broad variety of PEO-based polymers, such as PEO-based poly(meth)acrylates [21–26] and linear multi-block copolymers (poly(ether-ester)s [27–37], poly(ether-amide)s [19,21,38–49], poly(ether-urethane)s [50–55], poly(ether-siloxane-urethane) [56], poly(ether-urea)s [57], poly(ether-imide)s [58–72], poly(ether-sulfone)s [73,74]) have offered wide diversity of CO_2 separation performances from low permeability/high selectivity to high permeability/low selectivity membranes. These copolymers are particularly attractive for CO_2 post-combustion capture thanks to strong interactions between CO_2 and ethylene oxide (EO) units, providing high solubility contribution for CO_2 mass transport through PEO-based membranes. Moreover, the high mobility (glass transition temperature < room temperature) of amorphous PEO allowed to obtain membranes with high CO_2 diffusion coefficient.

Nevertheless, PEO exhibits high ability to crystallize, in particular for high PEO soft phase content, generating impermeable phases decreasing gas separation performances [66,75]. To reduce PEO crystallization, PEO-based multi-block copolymers were developed, alternating hard blocks, ensuring good membrane mechanical properties, with soft PEO-based blocks for CO_2 permeation. In order to further reduce soft block crystallization, other ether monomer units (propylene oxide PO, tetramethylene oxide TMO) were also considered in different soft polyether blocks (PPO, PTMO, or Jeffamines or Pluronics oligomers combining EO and PO units) [38,41,54,66,70,76].

Another successful approach for reducing PEO crystallinity in polymeric membranes for CO_2 capture consisted of developing grafted (or comb) copolymers with PEO-based grafts by grafting methods very different from the new grafting strategy described in this work. In the literature, several polymer backbones were considered such as polyvinyl polymers (poly(vinyl chloride) [77], poly((vinyl benzyl) trimethylammonium tetrafluoroborate [78], poly(vinyl trimethyl silane) [79], poly(vinyl imidazole) [80], poly(vinyl alcohol) [81], poly(meth)acrylic polymers (poly(methyl methacrylate) [82–84], poly(glycidyl methacrylate) [85], poly(acrylamide) [86], poly(2-(methacryloyloxy)ethyl-trimethylammonium tetrafluoroborate) [78], poly(sulfobetaine methacrylate) [87], poly(2-(4-benzoyl-3-hydroxy phenoxy) ethyl acrylate) [88]), major industrial rubbers (poly(styrene-block-butylene-block-styrene) SBS [89] and the corresponding hydrogenated rubber [90]), poly(1-trimethylsilyl-1-propyne [91]), polydimethylsiloxane [92], poly(ethylene-alt-maleic anhydride) [93] and polyethersulfone [94]. A few of the former grafted (or comb) copolymers with PEO-based grafts were

used as polymer matrices in high performance mixed-matrix membranes with different fillers (ZIF-8, UiO66-NH_2, bh-MgO, $FeCl_3$ etc.) [85,87,95,96] or facilitated transport membranes [97]. However, to the best of our knowledge, this type of grafting has not been reported for PEO-based multi-block copolymers so far, most likely due to their much more complex chemical structure.

Coming back to the literature on PEO-based multi-block copolymers of particular interest in this work, the influence of PEO content on CO_2 permeability does not obey a general rule and depends upon the chemical structure of the hard blocks and soft block crystallization [27,30,41,43,61,66,98,99]. When PEO crystallization was efficiently prevented in poly(ether-imide)s or poly(ether-urea-imide)s multi-block copolymers of particular interest in this new work, CO_2 permeability usually strongly increased with the PEO content while membrane selectivity decreased but still remained high for CO_2/N_2 separation in most cases [60,61,65,76]. In this view, it would be interesting to further increase the PEO content in these linear multi-block copolymers. However, in the different works reported so far, the PEO content remained limited to ca. 70 wt% for ensuring good membrane withstanding in operating conditions.

This work describes a new grafting strategy of PEO-based poly(urea-imide)s (PUIs) multi-block copolymers with PEO-based soft grafts, allowing to strongly push forward the limit of their soft polyether content while avoiding PEO crystallization for greatly improving their membrane properties. Compared to former literature on grafted/comb copolymers with PEO-based grafts, this new grafting strategy offers an advanced design of the grafted copolymers, by allowing the precise control of their structural parameters and a variation of their membrane properties over a very broad range. Furthermore, the use of PUIs provides specific advantages (better physical cross-linking and improved adhesion on different substrates for composite membranes) compared to related polyurethanes (PUs) or polyimides (PIs) [100,101].

The synthesis and physical-chemical characterization of a series of twelve original grafted multi-block PUI copolymers is first described. The grafting strategy involved a multi-step procedure based on step-growth polymerization, controlled radical polymerization (CRP) and Copper (I)-catalyzed Alkyne Azide Cycloaddition (CuAAC) "click" chemistry, providing a good control of grafting rate, graft molecular weight and resulting soft content. The grafting influence on the morphology of these new copolymers is then investigated based on different complementary characterizations. The third part reports their membrane properties for CO_2 sorption and pure permeation of CO_2 and N_2. Their correlation to the PUI chemical structure (grafting rate and graft length), morphology and soft content is then discussed to identify the key features to improve their membrane performance for CO_2 capture.

2. Experimental

2.1. Chemicals and materials

All chemicals were purchased from Sigma Aldrich unless specified otherwise. Jeffamine JFAED 2000, *4,4'*-Methylene-bis-phenylisocyanate (MDI, 98%), *4,4'*-(hexafluoro-*iso*-propylidene)-bis-(phthalic-anhydride) (6FDA, TCI, >98%), *N,N*-dimethylformamide (DMF, analytical reagent grade, 99.5%) and triethylamine (NEt_3, >99%) were purified following our former procedures [76,102]. Ethoxy di(ethylene glycol) acrylate monomer (EDEGA, >95%) was purified by vacuum distillation at 80 °C over benzoquinone. Tetrahydrofuran (THF, analytical reagent grade, 99.7%), copper (II) bromide ($CuBr_2$, 99%), copper (I) bromide (CuBr, 98%), tris[2-(diethylamino)amine] (Me_6TREN, 97%), and *N,N,N',N'',N''*-pentamethyldiethylenetriamine (PMDETA, 99%) were used as received. 2-Azidoethyl-2-bromoisobutyrate (AEBiB) (functional initiator with a terminal azido group) [103] and

4,4'-bis(hydroxymethyl)-1,6-heptadiyne (bisOHyne) (functional diol with two alkyne groups – Figure 1) [104,105] were synthesized according to the literature. For EDEGA controlled radical polymerization by Single Electron Transfer-Living Radical Polymerization (SET-LRP), the copper Cu(0) wire surface (3 cm length, 1.5 mm diameter) was activated using a former procedure [46].

2.2. Copolymers synthesis and characterization

2.2.1.Synthesis of PUI with alkyne side groups

This synthesis was carried out under dry inert atmosphere. In flask number ***1***, MDI (1.2 eq/ 1.668 g/6.67 mmoles) was added to a solution of JFAED 2000 (0.6 eq/ 6.668 g/3.33 mmoles) in 27 mL of dry DMF and reacted for 3 h at ambient temperature. In another flask (flask number ***2***), MDI (0.8 eq/ 1.112 g/4.44 mmoles) and bisOHyne (0.4 eq/ 0.338 g/2.22 mmoles) in 30 mL of dry DMF were reacted for 2h 30min at the same temperature. The content of flask number ***2*** was then transferred to flask number ***1*** and 20 mL of dry DMF were added for dilution before polycondensation with 6FDA (1 eq/ 2.468 g/5.55 mmoles). NEt_3 (2 eq/ 1.56 mL/11.1 mmoles) was used as catalyst for the chemical cyclization of imide groups with progressive rise in temperature (1 h 30 min at 60 °C and 8 h at 80 °C) for preventing side reactions of the alkyne groups. The purification of this new PUI (named PUI-g for PUI ready for grafting) was carried out according to the procedure we formerly reported for a related PUI, which did not contain alkyne side groups [76]. The final drying was operated under vacuum at 30°C for 24 h (yield of 85%). ^{1}H NMR (DMSO-d_6, 300 MHz) : δ : 1.02-1.23 ppm (q, 9.6 H, CH_3); 2.39 ppm (s, 1.6 H, CH_2); 2.96 ppm (s, 0.8 H, CH); 3.34-3.49 ppm (m, 52.3 H, CH_2); 3.7-4.1 ppm (m, 8.6 H, CH_2, CH); 5.9 ppm (d, 1.2 H, NH), 7-7.5 ppm (m, 16 H, CH); 7.6-8.2 ppm (d, 6 H, CH); 8.2-8.4 ppm (s, 1.2 H, NH); 9.5 ppm (d, 0.8 H, NH). SEC-MALLS (DMF + 2% w/v of LiCl): *dn/dC* = 0.12 mL/g; $\overline{M_n}$ = 94 380 g/mol, $\overline{M_w}$ = 266 400 g/mol, dispersity Đ = 2.8.

2.2.2.Synthesis of PEDEGA oligomers with an azido terminal group by SET-LRP

PEDEGA oligomers with an azido group for "click" chemistry were obtained by adapting our former procedure on the CRP of EDEGA acrylate monomer by SET-LRP [106]. In this work, the three different molecular weights (2000, 3600 and 5000 g/mol) targeted for the PEDEGA grafts were obtained by varying the ratios initiator/monomer/moderator/ligand AEBiB/EDEGA/$CuBr_2$/Me_6TREN as following: PEDEGA 2000: 1/9.5/0.05/0.2; PEDEGA 3600: 1/18/0.05/0.2 and PEDEGA 5000: 1/25/0.05/0.2. The N_3-PEDEGA oligomers were dried under vacuum at 60 °C. ^{1}H NMR ($CDCl_3$, 300 MHz) PEDEGA 2000: δ: 1.15-1.20 (m, 36 H, CH_3); 1.3-2.5 (m, 29.7 H, CH_2 and CH); 3.5-3.7 (m, 81 H, CH_2); 4.1-4.4 (m, 19.8 H, CH_2) ; PEDEGA 3600 : δ: 1.15-1.20 (m, 56.3 H, CH_3); 1.3-2.5 (m, 50.4 H, CH_2 and CH); 3.5-3.7 (m, 136.4 H, CH_2); 4.1-4.4 (m, 35.6 H, CH_2) ; PEDEGA 5000: δ: 1.15-1.20 (m, 81 H, CH_3); 1.3-2.5 (m, 75 H, CH_2 and CH); 3.5-3.7 (m, 204 H, CH_2); 4.1-4.4 (m, 50 H, CH_2). SEC-MALLS (THF): *dn/dC* = 0.068 mL/g; PEDEGA 2000 : $\overline{M_n}$ = 2004 g/mol, $\overline{M_w}$ = 2110 g/mol, dispersity Đ = 1.053 ; PEDEGA 3600 : $\overline{M_n}$ = 3444 g/mol, $\overline{M_w}$ = 4126 g/mol, dispersity Đ = 1.198 ; PEDEGA 5000 : $\overline{M_n}$ = 4780 g/mol, $\overline{M_w}$ = 4914 g/mol, dispersity Đ = 1.028

2.2.3.PUI grafting by "click" chemistry

PUI grafting was achieved by CuAAC "click" chemistry between alkyne-functionalized PUI and α-azido-functionalized PEDEGA oligomers, allowing different target grafting rates. In the following, we report the synthesis corresponding to the highest grafting rate (100%) and the longest grafts (PEDEGA5000). Azido-functionalized PEDEGA5000 (1.68 g; corresponding to 1 equivalent with respect to the alkyne side groups of PUI-g) and 4 mL of the PMDETA ligand were added to a solution

of 1g of PUI-g (containing 0.378 mmol of alkyne side groups) in 15 mL of distilled DMF. After three freeze-thaw cycles, the catalyst Cu(I)Br (54 mg; 1eq/alkyne group) was introduced under argon flow. After 48 h at 80 °C, the reaction medium was concentrated under vacuum and the crude grafted copolymer was precipitated in water in presence of the PMDETA ligand. The purification was carried out by three washings in water/PMDETA solutions. The soft elastomer copolymer PUI-g-1PEDEGA5000 was finally dried under vacuum at 40 °C overnight (yield: 78%). For ^{1}H NMR (DMSO-d_6, 300 MHz) see Results and Discussion.

2.3. Copolymer characterization

A Bruker Advance 300 spectrometer was used to obtain ^{1}H NMR spectra at 300.15 MHz for samples in DMSO-d_6 or $CDCl_3$ with TMS as a reference for the chemical shifts. Size exclusion chromatography with multi-angle laser light scattering (MALLS Wyatt Technology TREOS) was performed to determine the average molecular weights $\overline{M_n}$, $\overline{M_w}$ and dispersity Đ using our formerly reported procedure [76]. For characterizing PUI-g, 2 %w/v of LiCl was added to the DMF eluent for limiting polymer chain aggregation. The solvent used for SEC-MALLS characterization of the different PEDEGA oligomers was THF.

Differential scanning calorimetry (DSC) thermograms were recorded under nitrogen flow with a TA Instruments DSC Q2000 using a standard procedure formerly developed in our laboratory for characterizing other PUI copolymers [76]. The experimental error for the glass transition temperature (T_g) at midpoint was ca. 1°C. Polymer films of ca. 200 µm thickness were used for small-angle X-ray scattering (SAXS) characterization at the European Synchrotron Radiation Facility (ESRF) on the BM2D2AM beamline using the procedure formerly used for characterizing the corresponding linear multi-block PUI copolymers [76]. Membrane surface and cross-section images were obtained with a JEOL JSM-6490LV scanning electron microscope (SEM) at an accelerating voltage of 5 kV with magnification of 1.500 and 500, respectively. The membrane cross-sections were prepared by freeze-fracture by immersion in liquid nitrogen and then coated by gold-palladium. Transmission electron microscopy (TEM) was performed on a PHILIPS CM120 instrument at 80 kV. The different elastomer samples for TEM experiments were obtained by cryo-microtomy (80 nm thickness) and stained with Ruthenium tetraoxide vapors for 30 minutes.

2.4. Membrane casting

For each of the new polymer materials, 0.5 g of copolymer was dissolved in 20 mL of distilled DMF. Before casting on a Teflon mold, the copolymer solution was filtered on glass fibers. Most of the DMF was removed at 40 °C. The final membrane drying was achieved for 12h at 60 °C under vacuum. The membrane average thickness measured with an Elcometer™ was *ca.* 90 µm with a maximum standard deviation of 5 µm.

2.5. Sorption experiments

The magnetic suspension microbalance Rubotherm 2720 was used to perform the sorption experiments with high purity CO_2 gas (Messer, 99.995%) at different pressures at 35 °C. The CO_2 sorption was calculated from the constant mass (with a measurement error of ± 0.02 mg) obtained at sorption equilibrium by equation (1).

$$CO_2 sorbed\ (wt\ \%) = \frac{w_{eq} - w_{t0}}{w_{t0}} \times 100 \qquad (1)$$

where w_{eq} and w_{t0} are the sample weights after and before CO_2 sorption, respectively.

2.6. Gas permeability measurements

Time-lag experiments were carried out at 35 °C and an upstream pressure of 2 bar, after drying the membranes under vacuum overnight in the time-lag cell. Pure gases CO_2 (Messer, 99.995%) and N_2 (Messer, 99.995%) were used for the gas permeation experiments. The equipment and procedure have already been described for characterizing the corresponding linear multi-block copolymers [76]. The membrane performance was characterized by gas permeability *P* and ideal separation factor $\alpha_{CO2/N2}$ based on five experiments for each membrane sample (equations (2) and (3)):

$$P = \frac{J_{st} * l}{P_{upstream}} \quad (2)$$

where l is the average thickness of the active membrane area and J_{st} is the gas obtained for the steady state of gas permeation. In equation 2, the unit of the steady-state flux J_{st} is cm^3 (STP).cm^{-2}.s^{-1} for allowing a calculation of gas permeability in Barrer.

$$\alpha_{CO2/N2} = \frac{P_{CO2}}{P_{N2}} \quad (3)$$

The diffusion coefficient *D* was estimated from the time-lag θ corresponding to the gas breakthrough time across the membrane (equation (4)). The sorption coefficient S was then deduced from equation (5) corresponding to the solution-diffusion model [107] :

$$D = \frac{l^2}{6\theta} \quad (4)$$

$$P = D * S \quad (5)$$

3. Results and discussion

3.1. Synthesis and characterization of the grafted PEO-based PUI copolymers

3.1.1. Synthesis of the grafted PEO-based PUI copolymers

The synthesis of the new grafted copolymers (Fig. 1) started by incorporating alkyne side groups into the best PEO-based PUI multi-block copolymer reported in our former work on CO_2/N_2 separation membranes [76]. The resulting functionalized copolymer (PUI-g) was a PUI "graftable" by CuAAC "click" chemistry. The synthesis of PUI-g involved the reaction of PU macrodiisocyanates with an fluorinated aromatic dianhydride (6FDA) following a fairly uncommon route for polyimide synthesis allowing great structure variability [100,108–115]. In a first step, two different macrodiisocyanates were prepared independently from reactions between a PEO-based diamine (Jeffamine JFAED 2000) and an aromatic diisocyanate (MDI), and a diol containing two alkyne side groups (BisOHyne) and MDI. The use of the Jeffamine for the copolymer synthesis was motivated by the results obtained in our former work on related PEO-based PUI linear multi-block copolymers, having shown the absence of crystallization of the corresponding Jeffamine soft segments in these polymer materials [76]. Furthermore, this two-pot strategy was chosen to compensate for the difference in nucleophilicity of the diamine and diol monomers. It avoided using toxic tin-based catalysts and ensured the success of the synthesis. These macrodiisocyanates were then brought together and were reacted with 6FDA by step-growth polymerization. This specific dianhydride was chosen for promoting the copolymer solubility in dipolar aprotic solvents (*e.g.*, DMF) necessary for its grafting.

The grafted PUIs were then obtained by CuAAC "click" chemistry (step 3) between PUI-g containing alkyne side groups and PEDEGA CO_2-philic grafts bearing a terminal azido group. These α-azido-

functionalized PEDEGA grafts were obtained by SET-LRP controlled radical polymerization using a functional azido initiator to provide the terminal azido group. Relatively low molecular weights of PEDEGA grafts were chosen for ensuring high grafting efficiency. SET-LRP ensured a good control of the graft molecular weight from 2000 to 5000 g/mol as shown by their low molecular weight dispersity. The grafting rate (defined as the percentage of the PUI-g alkyne groups grafted by "click" chemistry) was varied between 25 to 100%, leading to a broad range of soft contents in the grafted copolymers. The name chosen for the grafted copolymers was PUI-g-XPEDEGAY with *X* being the grafting rate (%)/100 and *Y* the molecular weight (in g/mol) of the PEDEGA grafts. For simplicity, the series of the copolymers grafted with different grafting rates of PEDEGA Y was named PUI-g-PEDEGAY.

For pervaporation membranes for ETBE biofuel purification [103], we had reported the synthesis of other grafted PUI copolymers from a different precursor PUI and with different grafts, which were polymethacrylate oligomers obtained by ATRP controlled radical polymerization. In this new work, the precursor PUI is original and contains a monomer unit (bisOHyne) with two alkyne side groups allowing the straightforward grafting by "click" chemistry and playing a particular role for the morphology developed by the new grafted copolymers as discussed later in section 3.1.3. The use of this new monomer unit has the great advantage of saving one synthesis step compared to our earlier grafting route. Moreover, in this work, the chemical structure of the grafts has also been changed for PEO-based polyacrylate oligomers to provide much better properties for CO_2 permeation. These polyacrylate oligomers were obtained by another controlled radical polymerization (SET-LRP, which is better adapted to acrylate monomers), by extending the approach we had formerly developed for the synthesis of pseudopeptide bioconjugates for CO_2 capture [106]. In this work, new PEDEGA oligomers with different molecular weights were synthesized to vary the graft length, leading to 3 series of twelve original grafted PUI copolymers with different grafting rates and graft lengths (Table 1).

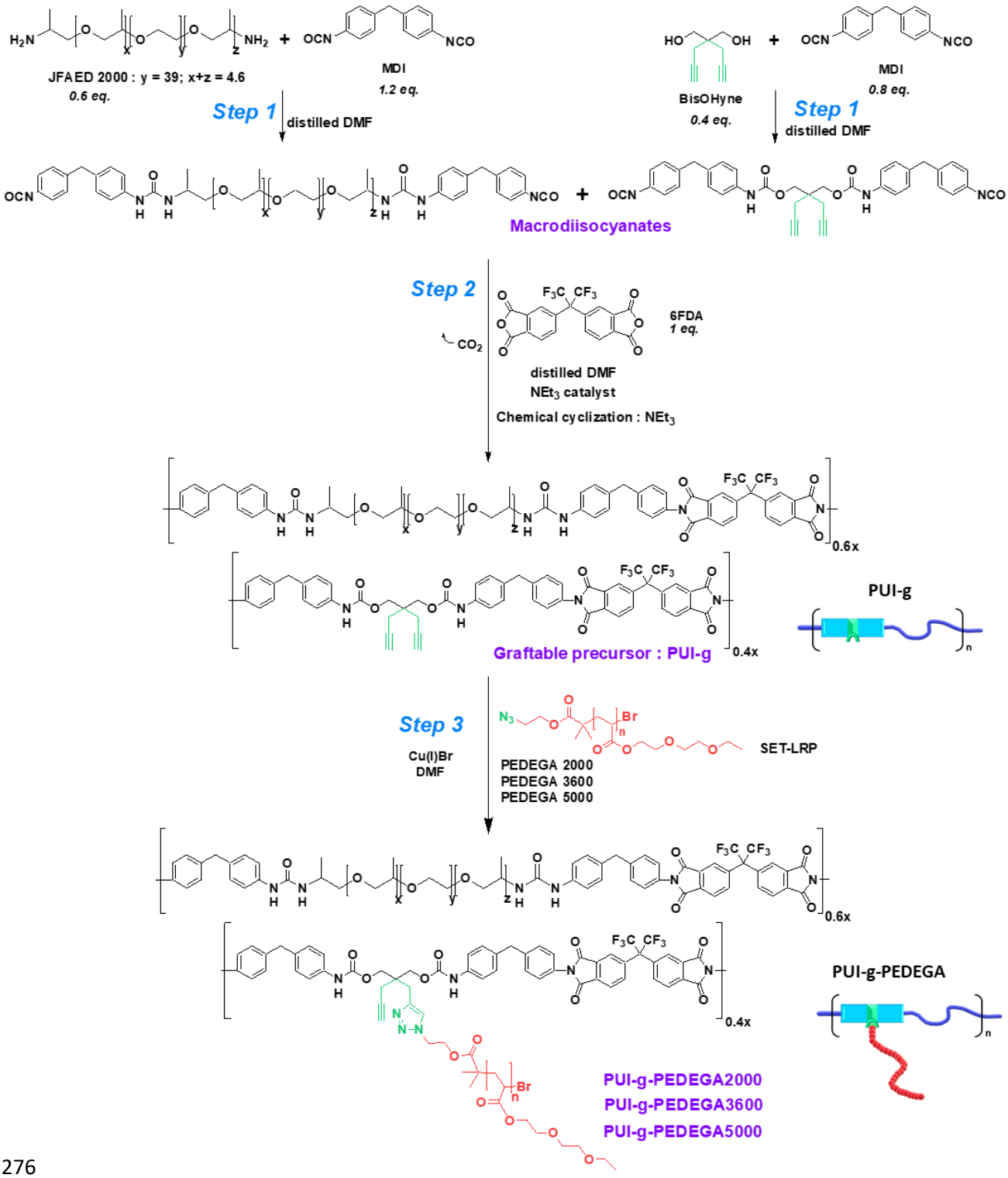

Fig. 1. Synthesis of the graftable precursor PUI-g by step-growth polymerization (steps 1 and 2) and grafting with soft grafts PEDEGA (step 3).

3.1.2. Physical chemical characterization of the grafted PEO-based PUI copolymers

Characterization by ^{1}H NMR enabled to validate the chemical structure of PUI-g and that of the grafted PUIs and to calculate their experimental grafting rate. As an example, Fig. 2 shows the proton identification of PUI-g, PEDEGA 5000 grafts and the grafted copolymer PUI-g-1PEDEGA5000. Monomers stoichiometry in PUI-g (JFAED 2000 (0.6) + BisOHyne (0.4)/MDI (2)/6FDA(1)) was

checked using protons peak integrations, which also confirmed the expected amount of alkyne side groups in PUI-g. The spectrum of the grafted multi-block copolymer PUI-g-1PEDEGA5000 exhibited ^{1}H NMR signals coming from both PUI-g and PEDEGA 5000. SEC-MALLS was also used to qualitatively verify the efficiency of the copolymer grafting (see Fig. S1). The grafting rates *GR* were calculated from integration area A_1 of CH_3 protons of JFAED 2000 propylene oxide units and CH_3 protons of PEDEGA grafts (δ: 1.15-1.20 ppm : D, I, m on Fig. 2) and integration area A_2 corresponding to CH protons of MDI and CH protons of triazole ring (δ: 7-7.5 ppm : A, a, b, d, e on Fig. 2) by solving equation 6.

$$\frac{A_1}{A_2} = \frac{0.6 \times (3 + 5.16 \times 3) + 0.4 \times 2 \times (\frac{GR}{100}) \times (6 + 3 \times \overline{X_{nPEDEGA}})}{0.6 \times 2 \times 8 + \ 0.4 \times 2 \times 8 + 0.4 \times 2 \times (\frac{GR}{100})} \quad (6)$$

with $$\overline{M_{nPEDEGA}} = \ M_{AEBiB\ initiator} + \overline{X_{nPEDEGA}} \times M_{EDEGA} \quad (7)$$

In equation 7, $\overline{M_{nPEDEGA}}$ is the number-average molecular weight of the PEDEGA grafts determined by SEC-MALLS analysis, and $\overline{X_{nPEDEGA}}$ is the corresponding number-average degree of polymerization. M_{EDEGA} is the molecular weight of the EDEGA monomer unit and $M_{AEBiB\ initiator}$ is the molecular weight of the AEBiB initiator used for the synthesis of the azido-PEDEGA oligomers.

Table 1 shows that the experimental grafting rates were very close to the theoretical ones for all the grafted copolymers. Therefore, very high grafting efficiencies were obtained in this work (Table 1 – column 4) and the copolymer/graft coupling by CuAAC "click" chemistry was quantitative. Therefore, all the PEDEGA grafts introduced in the reaction medium were effectively grafted onto PUI-g ensuring the control over the number of grafts in the grafted copolymers.

The very high grafting efficiency also enabled to control the grafting rate very easily from 25% to 100%, resulting in soft contents varying in a very broad range from 57 to 85 wt% (Table 1 - last column). The soft content for each grafted copolymer was then calculated from the corresponding grafting rate *GR* and PEDEGA graft number-average molecular weight $\overline{M_{nPEDEGA}}$ according to equation 8 and reported in Table 1. Consequently, the new grafting strategy enabled to increase the maximum PUI soft content from 70 wt% in our former work on PUI multi-block copolymers to the very high content of 85 wt% for the grafted PUI multi-block copolymer PUI-g-1PEDEGA5000 corresponding to the highest grafting rate and the highest PEDEGA graft molecular weight.

$$Soft\ content\ (wt\%) = \frac{0.6 \times M_{JFAED2000} + 0.4 \times 2 \times (\frac{GR}{100}) \times \overline{M_{nPEDEGA}}}{M_{repeating\ unit\ of\ grafted\ copolymer}} \times 100 \quad (8)$$

with $$M_{repeating\ unit\ of\ grafted\ copolymer} = \ 0.6 \times M_{JFAED2000} + 0.4 \times M_{bisOHyne} + 0.4 \times 2 \times \left(\frac{GR}{100}\right) \times \overline{M_{nPEDEGA}} + 2 \times M_{MDI} + \ M_{6FDA} - 2\ M_{CO2} \quad (9)$$

In equation 9, $M_{repeating\ unit\ of\ grafted\ copolymer}$ is the molecular weight of the repeating unit of the grafted copolymer and M_i the molecular weight of species *i*.

Table 1. Grafting rate, grafting efficiency and soft content of PUI-g and grafted PUIs, with PUI-g-XPEDEGAY: X the grafting rate/100 and Y the molar mass of PEDEGA grafts.

Sample	Theoretical grafting rate (%)	Experimental grafting rate (%)	Grafting efficiency (%)	Soft content (wt %) (^{1}H NMR)

		(^{1}H NMR)	(^{1}H NMR)	
PUI-g	-	-	-	57
PUI-g-0.25PEDEGA2000	25	24	96	64
PUI-g-0.5PEDEGA2000	50	49	98	69
PUI-g-0.75PEDEGA2000	75	76	100	72
PUI-g-1PEDEGA2000	100	101	100	75
PUI-g-0.25PEDEGA3600	25	24	96	68
PUI-g-0.5PEDEGA3600	50	51	100	74
PUI-g-0.75PEDEGA3600	75	75	100	79
PUI-g-1PEDEGA3600	100	100	100	82
PUI-g-0.25PEDEGA5000	25	26	100	71
PUI-g-0.5PEDEGA5000	50	50	100	78
PUI-g-0.75PEDEGA5000	75	75	100	82
PUI-g-1PEDEGA5000	100	100	100	85

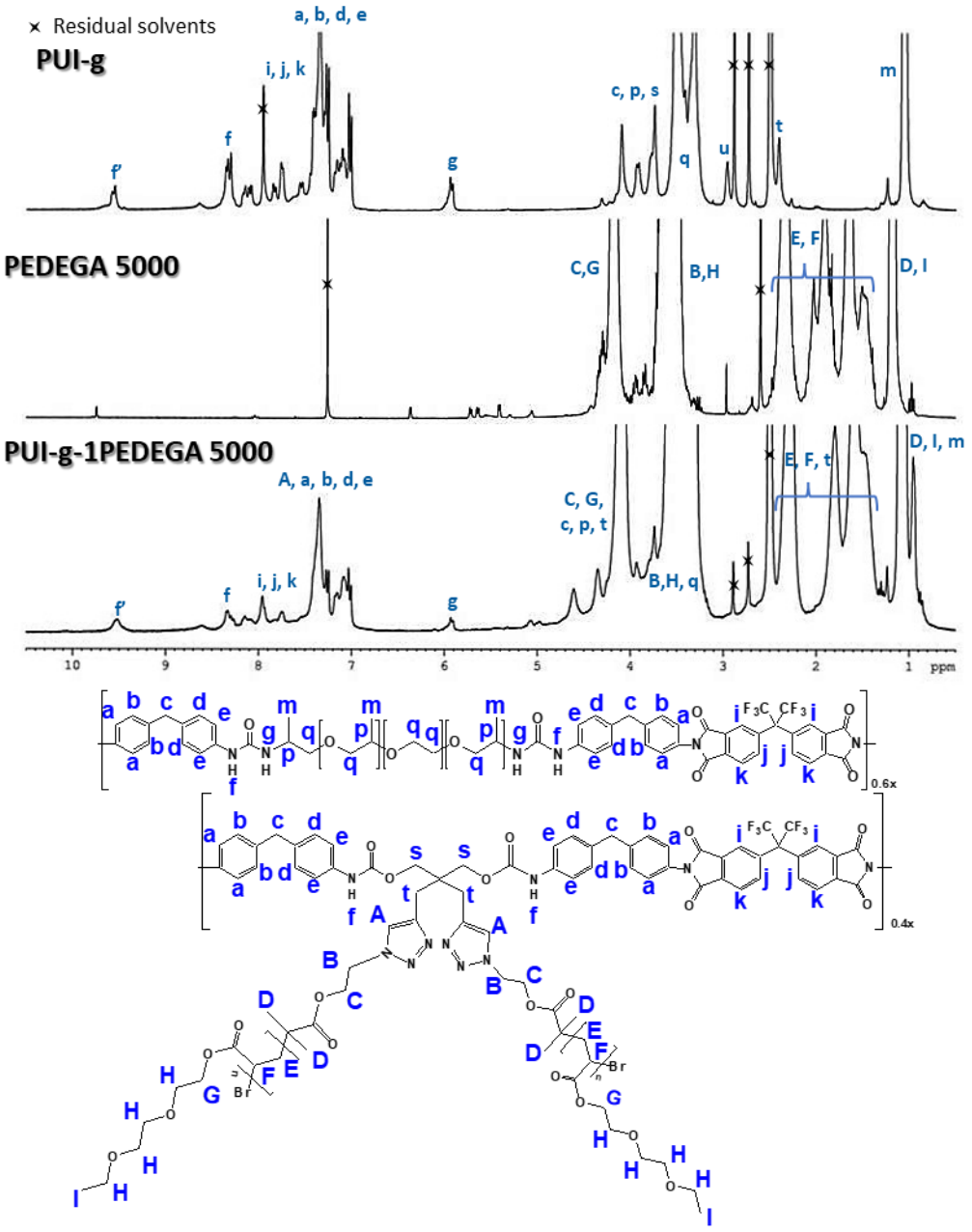

Fig. 2. ^{1}H NMR characterization of PUI-g, soft graft PEDEGA 5000, and PUI-g-1PEDEGA5000 (copolymer with maximum grafting rate and graft molecular weight taken as way of example).

3.1.3. Morphology characterization for the PEO-based grafted PUI multi-block copolymers

Multi-block (segmented) copolymers have complex morphology and this morphology has a great influence on their permeability and membrane properties [33,38,40,116]. In this context, reducing the fraction of crystalline phases remains a major challenge for the design of high-performance membranes [27,33,40,66]. In these copolymers, the soft and hard blocks can be fully mixed, partially mixed or separated, depending on the chemical structure and molecular weight of these blocks. The best membrane properties are usually obtained when the quasi-impermeable hard blocks are excluded from the soft blocks, which corresponds to strong phase separation also ensuring good material physical cross-linking [27,33,40,66]. In the following, the morphology of the new grafted copolymers was assessed by complementary techniques in comparison with that of their precursor PUI-g.

Fig. 3 shows the DSC thermograms for PUI-g and the grafted PUI multi-block copolymers displayed in three series of data corresponding to different graft molecular weights (PEDEGA 2000, 3600 and 5000) and grafting rates varying from 25 to 100%. In all of these thermograms, the glass transition temperature T_g of the hard blocks was not observed because the DSC scanning temperature has been limited to prevent the chemical degradation of the PEO-based soft blocks, as also reported in earlier works on other PEO-based polyimides [59,61,66,76]. For PUI-g, the T_g of −25°C was well below ambient temperature, meaning that the JFAED 2000 soft blocks formed a soft rubbery phase. However, this T_g was much higher than that of the JFAED 2000 oligomer (T_g = −65°C) due to the constraints imposed by the hard blocks representing almost half of the copolymer weight. Compared to the corresponding multi-block copolymer JFAED2000/MDI/6FDA (T_g = −39°C) containing only 30 wt% of hard blocks reported in our former work [76], the T_g of PUI-g was higher, as expected from its much higher hard block content (43 wt%).

For the grafted PUI copolymers, a unique glass transition *for the soft phase* was observed in each thermogram, evidencing the presence of only one soft phase composed by JFAED 2000 soft blocks and PEDEGA grafts (Fig. 3). For the shortest grafts (PEDEGA 2000), the T_g of ca. −25 °C remained almost identical to that of PUI-g (Table 2), showing that the soft phases exhibited comparable dynamics in both non-grafted copolymer and multi-block copolymers grafted with the shortest PEDEGA grafts. However, when the length of the PEDEGA grafts was increased (PEDEGA 3600 and 5000), the T_g was strongly decreased to −46 °C. Therefore, the grafting with longer PEDEGA grafts allowed shifting the T_g towards the T_g of the corresponding PEDEGA oligomers (T_g = −50°C) and strongly improved the mobility of the corresponding soft phase. For any given graft length, the grafting rate (GR) was not found to have significant impact on the polymer glass transition dynamics for GR above 25%. Therefore, for the longest grafts (PEDEGA 3600 and 5000), the grafting of the first grafts induced the spacing of the macromolecular backbone and generated a constant microenvironment for the soft phase. However, as expected, the values of ΔC_p associated to the glass transition of the grafted multi-block copolymers (which is related to the weight of the soft phase undergoing the glass transition) increased with their soft phase content (Table 2 – column 4). The thermograms obtained for PUI-g-PEDEGA3600 showed a secondary glass transition at ca. −25 °C (*i.e.* the T_g of PUI-g). However, this glass transition corresponded to a very small ΔC_p compared to the main glass transition, involving that the corresponding soft phase was very limited compared to that developed by the mixing of the soft blocks and grafts.

Furthermore, the absence of crystallinity was observed in the thermograms of all the PUI copolymers, with no melting endotherms even for the highest soft contents. Therefore, the Jeffamine soft segments did not crystallize in the new grafted copolymers, as it was also observed for the related linear multi-block copolymers reported in our former work [76]. This was due to the particular structure of the Jeffamine, whose propylene oxide units prevented crystallization. In addition, the PEDEGA grafts did not crystallize either, in good agreement with former works on other grafted (or comb) copolymers with related PEO-based poly(meth)acrylate grafts [77,80,92,95]. In conclusion, DSC experiments showed that the new grafted multi-block architecture allowed to obtain membrane materials with very high PEO-based soft phase content (up to 85 wt%) without crystallinity, which is a strong advantage for gas permeation.

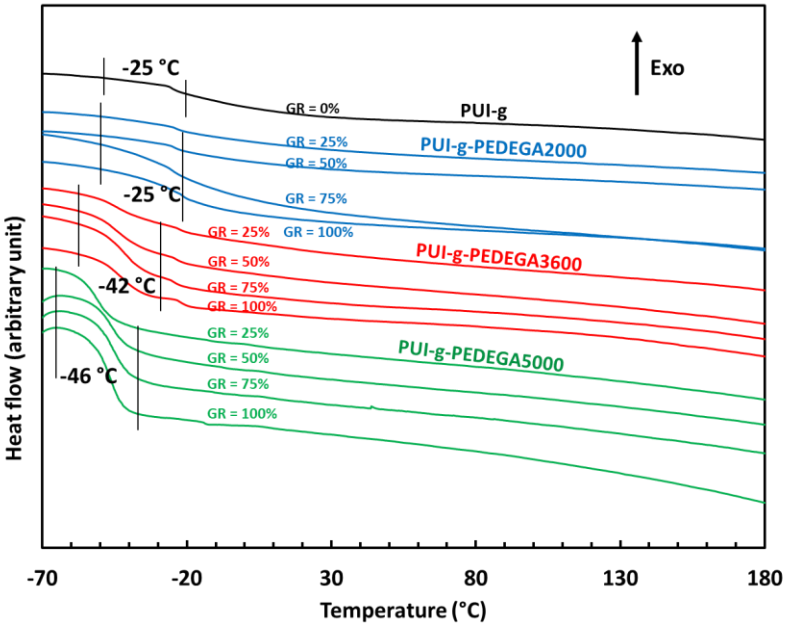

374

375 **Fig. 3 Thermograms of PUI-g and grafted PUI multi-block copolymers with different lengths of grafts (PEDEGA**
376 **2000, 3600 and 5000) and different grafting rates (GR) from 25 to 100% (second heating – 10°C/min). Note: The**
377 **thermograms have been shifted for improved visualization and correspond to arbitrary heat flow values.**

378 **Table 2. DSC results of PEDEGA oligomers and grafted PUI multi-block copolymers (second heating – 10°C/min).**

Sample	Soft phase content (%)	Tg (°C)	ΔCp (J/(g.°C))
JFAED 2000 [76]	-	-65	0.20
PEDEGA 2000	-	-50	0.66
PEDEGA 3600	-	-49	0.74
PEDEGA 5000	-	-51	0.75
PUI-g	57%	-25	0.33
PUI-g-0.25PEDEGA2000	64%	-23	0.33
PUI-g-0.5PEDEGA2000	69%	-24	0.35
PUI-g-0.75PEDEGA2000	72%	-25	0.36
PUI-g-1PEDEGA2000	75%	-25	0.45
PUI-g-0.25PEDEGA3600	68%	-45	0.35
PUI-g-0.5PEDEGA3600	74%	-45	0.42
PUI-g-0.75PEDEGA3600	79%	-41	0.44
PUI-g-1PEDEGA3600	82%	-42	0.50
PUI-g-0.25PEDEGA5000	71%	-46	0.40
PUI-g-0.5PEDEGA5000	78%	-47	0.44
PUI-g-0.75PEDEGA5000	82%	-46	0.51
PUI-g-1PEDEGA5000	85%	-46	0.55

379

380

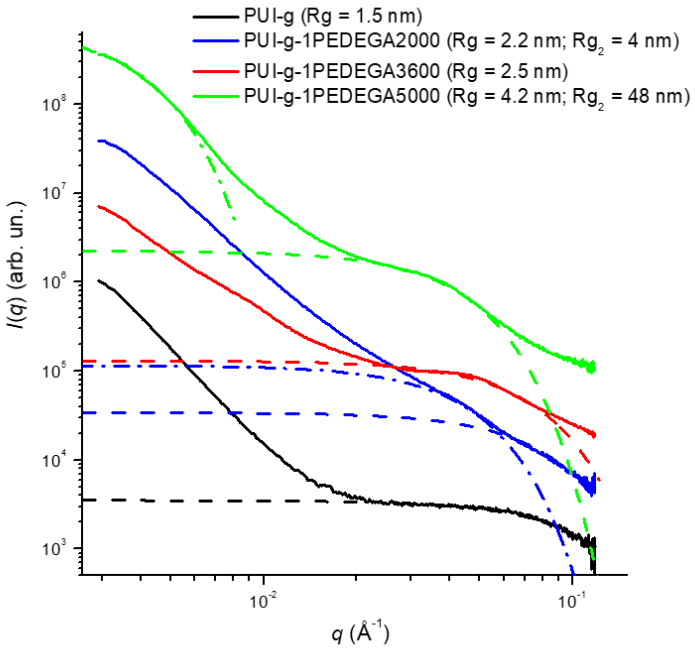

Fig. 4 - Influence of soft grafts molecular weight on SAXS experiments for the PUI copolymers grafted with maximum grafting rate (100%) and their precursor PUI-g.

The morphology at the nanoscale was investigated by synchrotron SAXS and TEM experiments for the highest grafting rate (100%) for each graft length (PEDEGA 2000, 3600 and 5000), corresponding to the best membrane materials of each series of grafted copolymers, and compared with that of the precursor PUI-g. For PUI-g, the SAXS pattern (Fig. 4) showed the same type of nano-structuration of the hard blocks as that observed for the corresponding linear PUI based on the same soft blocks JFAED 2000 in our previous work [76]. The analysis of the SAXS pattern with the Guinier's law for isometric particles ($I(q)=I_o\exp(-R_o^2q^2/3)$) at high q values led to a gyration radius of 1.5 nm (in comparison with 2 nm in our former work [76]) for the hard block domains. Fig. 4 shows that the corresponding shoulder is shifted towards the lower q-range for the grafted copolymers. Accordingly, the use of Guinier's law led to gyration radius for the hard block domains, with very small sizes varying from 2.2 nm to 4.2 nm. As the grafting sites were strategically located on the aromatic/aliphatic hard blocks based on the new monomer unit (bisOHyne) (which correspond to 40 mol% of the hard blocks as shown in Fig. 1), grafting induced the swelling of the hard block nanodomains as shown by the increase of the corresponding gyration radii compared to that of the PUI-g precursor. Furthermore, all systems displayed an increase of scattered intensity in the low q range, indicative of larger scale fluctuations in the repartition of hard and soft phases. In particular, for PUI-g-1PEDEGA5000 corresponding to the longest grafts and to the extreme soft content of 85 wt%, the SAXS pattern obtained in the low q-range ($q < 4.\ 10^{-3}$Å^{-1}) showed the beginning of another shoulder resolved in the assessable q-range, corresponding to a gyration radius of the order of 48 nm. For the corresponding TEM analyses, the preparation of the samples by cryo-ultramicrotomy was particularly difficult for the grafted copolymers due to their high soft contents and led to some shadows on the corresponding TEM pictures (Fig. 5). Nevertheless, the TEM images showed fine dark nanodomains with characteristic sizes of less than 5 nm (in good agreement with the SAXS results) corresponding to the stained hard blocks. The TEM images also showed that their dispersion in the soft phase increased with the PEDEGA graft length. This dispersion was related to the dragging of hard blocks induced by the covalent grafting of the PEDEGA grafts on the aromatic/aliphatic hard

blocks. In accordance with the SAXS experiments, the TEM image of PUI-g-1PEDEGA5000 revealed unstained/clear soft nanodomains with characteristic dimensions of the order of 50 nm. Fig. 6 schematically illustrates the morphology of PUI-g and the grafted copolymers with the shortest and longest PEDEGA grafts as deduced from the SAXS and TEM experiments. The grafting induced the expansion of the soft content, along with the dragging of some hard blocks in the soft phase (PUI-g-1PEDEGA2000). The longer the grafts, the greater the soft content and dragging of these hard blocks in the soft phase (PUI-g-1PEDEGA5000).

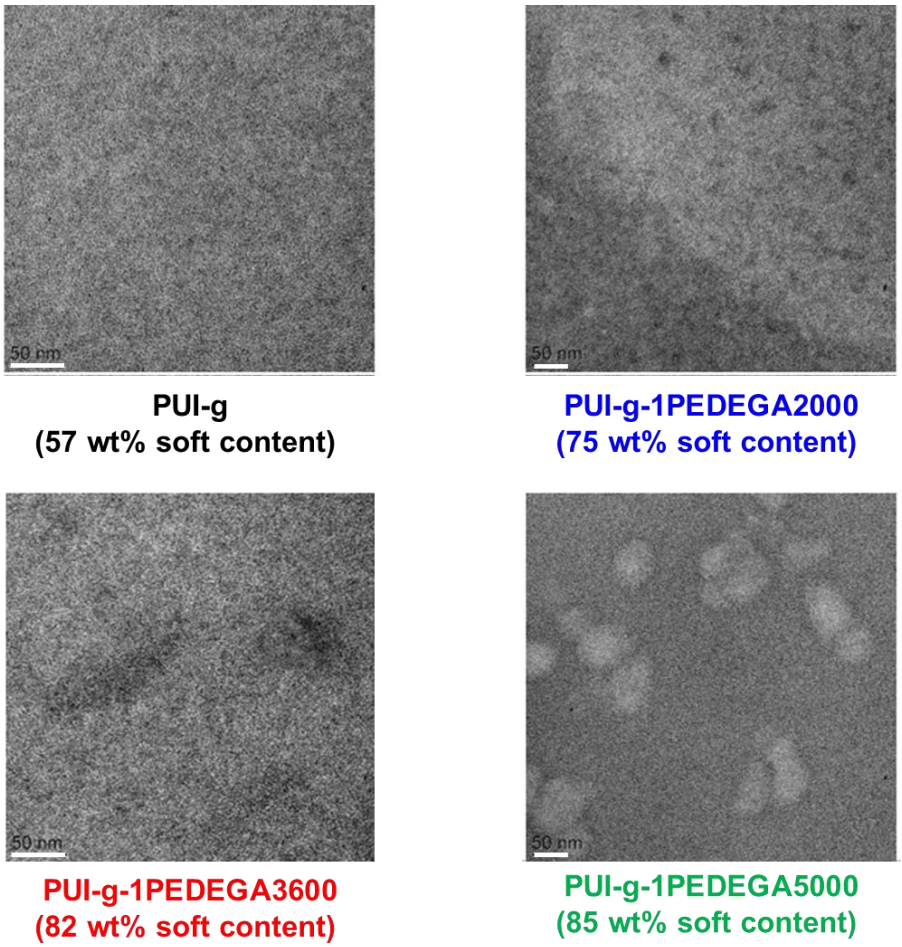

Fig. 5. Influence of soft grafts molecular weight on TEM images of the PUI copolymers grafted with maximum grafting rate (100%) and their precursor PUI-g. Note: the white scale represents 50 nm.

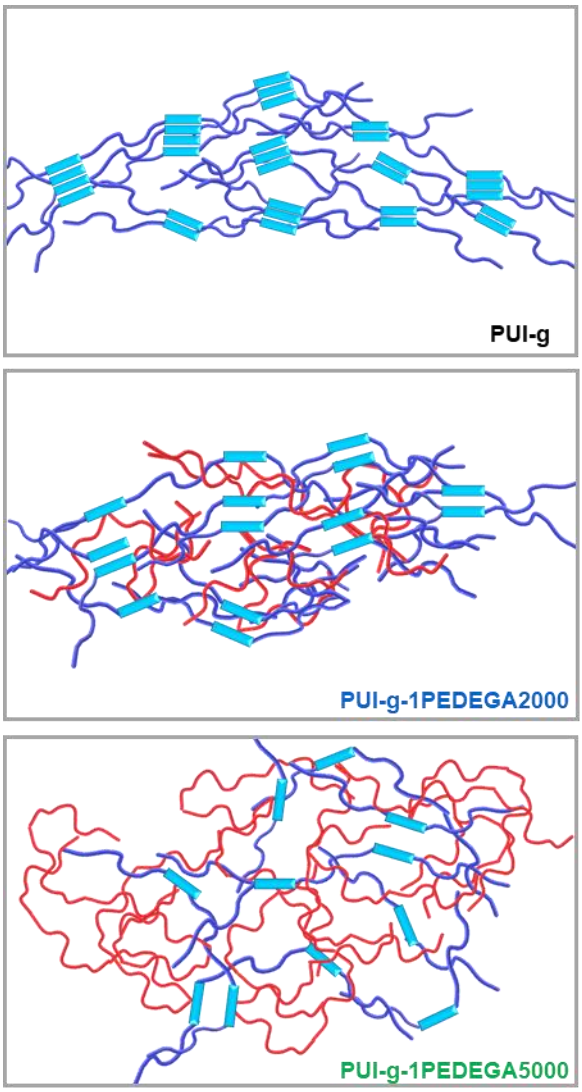

Fig. 6. Schematic illustration of the influence of soft grafts molecular weight on morphology of the grafted PUI copolymers with the maximum grafting rate (100%)

3.1.4. CO_2 sorption properties

The CO_2 mass uptake at sorption equilibrium of the different copolymers was assessed at 35 °C with increasing CO_2 pressures between 0 and 10 bar in a microbalance. Fig. 7 shows the influence of PEDEGA soft grafts molecular weight on the CO_2 sorption isotherms of the grafted PUI copolymers with maximum grafting rate (100%) and their precursor PUI-g. The sorption isotherms for all the membrane materials were linear and characteristic for Henry dissolution typical for rubbery polymers. Linear CO_2 isotherms have also been reported for other PEO-based linear multi-block copolymers (Polyactive 3000 and 4000) at high temperatures (50-70°C) ensuring the melting of the PEO crystallites although a deviation from Henry's law was observed at lower temperatures corresponding to semi-crystalline PEO blocks [37]. In this work, the grafted copolymers were non-crystalline due to the use of JFAED 2000 and their particular grafted copolymer structure, and Henry's law was followed even at relatively low temperature (35°C). At the pressure of 2 bar chosen for the gas permeation experiments, a relatively low amount of CO_2 (ca. 1 wt%) was absorbed in the grafted multi-block copolymers and their precursor PUI-g. However, for each CO_2 pressure, the CO_2 mass

uptake increased with the graft length and soft phase content up to 5.6 wt% at 10 bar for the best grafted PUI multi-block copolymer (PUI-g-1PEDEGA5000) corresponding to the longest grafts and highest soft content.

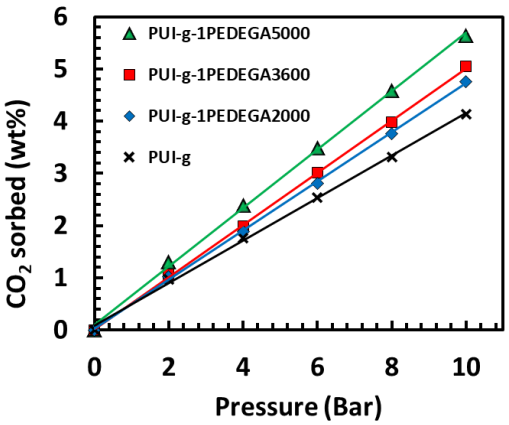

Fig. 7. Influence of soft grafts molecular weight on CO_2 sorption isotherms of the PUI copolymers grafted with maximum grafting rate (100%) and their precursor PUI-g at 35°C.

3.1.5. CO_2 permeation properties

The CO_2 permeation properties of the grafted copolymers and their precursor PUI-g were determined for the pure gases CO_2 and N_2 at 2 bar and 35 °C referring to usual conditions for CO_2 capture [33,99]. The membranes were dense (no pores) with thicknesses of ca. 90 µm as shown by SEM experiments (Fig S2). The membrane thicknesses used for gas permeability calculations were measured with an Elcometer micrometer and averaged on the active surface area for each membrane. Pure gas experiments were performed in this study because former works on other PEO-based multi-block copolymers have shown that their permeation properties were almost the same for mixed-gas separation [75,117]. Because of the mild conditions of CO_2 capture from flue gas, with moderate feed pressure and relatively low CO_2 content in feed mixture (5-14%), the CO_2 partial pressure is low. These conditions generally lead to relatively low CO_2 sorption (as also found in this work) and very limited plasticizing of such copolymers [75,117].

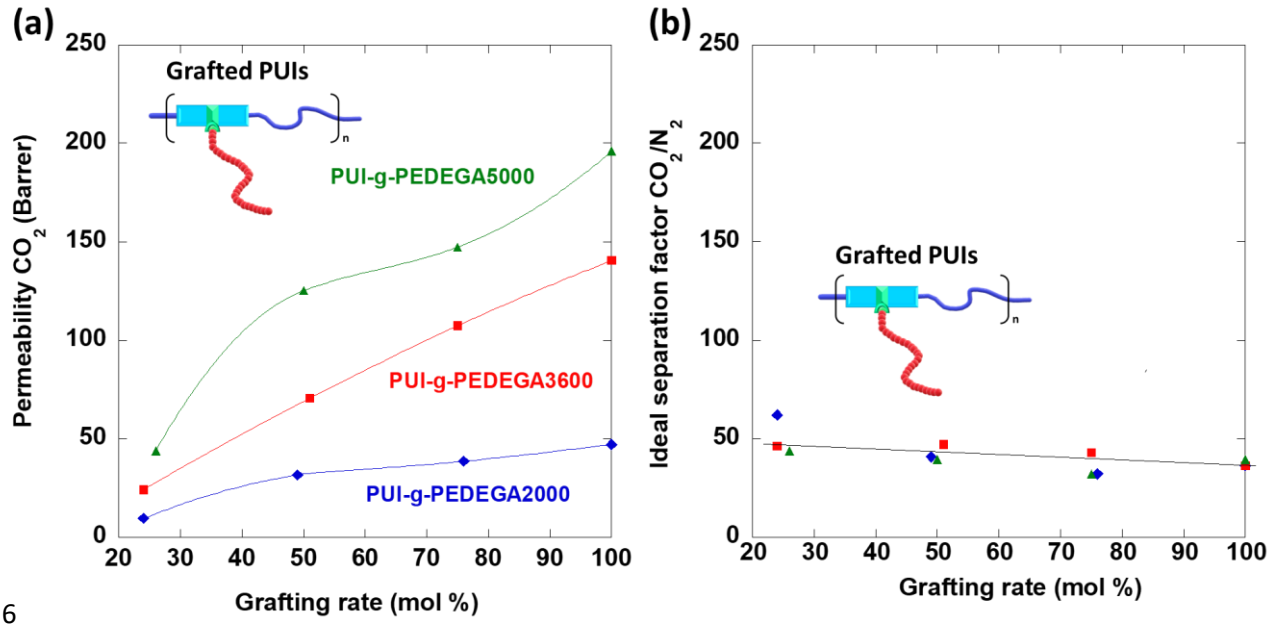

Fig. 8. Influence of grafting rate on (a) permeability of CO_2 and (b) ideal separation factor $\alpha CO_2/N_2$ for the grafted PUI copolymers at 2 bar and 35°C.

Fig. 8 shows the influence of grafting rate on CO_2 permeability and ideal separation factor $\alpha CO_2/N_2$ for three series of grafted multi-block copolymers with increasing PEDEGA graft molecular weight from 2000 to 5000 g/mol. The CO_2 permeability increased with the grafting rate for all the grafted copolymers (Fig. 8a). When the PEDEGA graft molecular weight was increased, the increase of CO_2 permeability was further improved because of the stronger contribution of the longer PEDEGA grafts to the soft phase content. Globally, the grafting strategy greatly increased CO_2 permeability from 11.5 Barrer for the precursor PUI-g to 196 Barrer for the best grafted multi-block PUI copolymer PUI-g-1PEDEGA5000, corresponding to the highest grafting rate (100%) and PEDEGA graft molecular weight (5000).

At the same time, the ideal separation factor $\alpha CO_2/N_2$ was maintained at a high level close to 40 for all the grafted copolymers, whatever their grafting rate and PEDEGA graft molecular weight (Fig. 8b). The CO_2 sorption coefficients slightly increased with the grafting rate and PEDEGA graft molecular weight and the N_2 sorption coefficients were extremely low for all these membranes, corresponding to very high ideal sorption selectivity also reported for other PEO-containing copolymers [15,17,71] (Table S1 – Supporting information). However, the variation of CO_2 sorption coefficients with the copolymer structural parameters was much lower than that of the CO_2 diffusion coefficients, which increased over almost one order of magnitude within the range of study. Therefore, diffusion increase was mainly governing improvement in gas permeation through these membranes due to the increase in their soft content. This trend was also in good agreement with former works on other PEO-based multi-block copolyimide membranes for CO_2 separations [58,63,70,72,98].

To highlight the specific interest of the grafting strategy developed in this work, Fig. 9 compares the membrane properties of the grafted PUI copolymers with those of related linear PUI multi-block copolymers previously reported in our former work [76]. The linear PUI multi-block copolymers exhibited a chemical structure comparable to that of the grafted PUI copolymers, with hard blocks made of MDI/6FDA monomer units, and JFAED soft blocks with increasing molecular weights from

600 to 2000 g/mol (corresponding to soft phase contents increasing from 41 to 70 wt%, respectively). Fig. 9a shows that the CO_2 permeability of the linear PUI copolymers increased exponentially from 2 Barrer to 57 Barrer when their soft content was increased from 41 to 70 wt%, which was the maximum soft content allowed for the linear PUI copolymers. Such drastic permeability increase was previously related to the separation of their soft and hard blocks for the highest soft content with percolation of a soft elastomer phase [76]. At the same time, the ideal separation factor $\alpha CO_2/N_2$ of the linear PUI multi-block copolymers strongly decreased with their soft content from 207 to 50 Barrer. Therefore, the CO_2 permeability of the linear PUI copolymers was strongly restricted by a permeability-selectivity trade-off, albeit still displaying high selectivity for CO_2/N_2 separation.

The grafting strategy enabled to overcome the soft content limitation of the linear PUI copolymers by allowing much higher soft contents up to 85 wt%. For each series of grafted copolymers, CO_2 permeability increased linearly with the copolymer soft content. The same type of linear permeability increase has been reported for different multi-block copolymers and it is generally ascribed to some intermixing between the soft and hard blocks as reviewed in a former work [118]. In this new work, the linear permeability increase relates to the special morphology developed by the grafted PUI copolymers, involving the dragging of the hard blocks bearing the PEDEGA grafts within the soft phase (as explained in section 3.1.3). In the grafted PUI copolymers, both CO_2 and N_2 diffusivity increased due to their soft content increase (Table S1 – Supporting information). However, the hard blocks mixed within the soft phase acted as impermeable obstacles and contributed to limit the increase in the diffusion coefficients of the gas molecules and, consequently, to limit the decrease in membrane ideal separation factor, which was maintained at high level even for the highest soft contents (Fig. 9b). Therefore, the special morphology of the new membranes allowed a CO_2 permeability increase by a factor of 17 with quasi-constant membrane selectivity ($\alpha CO_2/N_2$ of ca. 40).

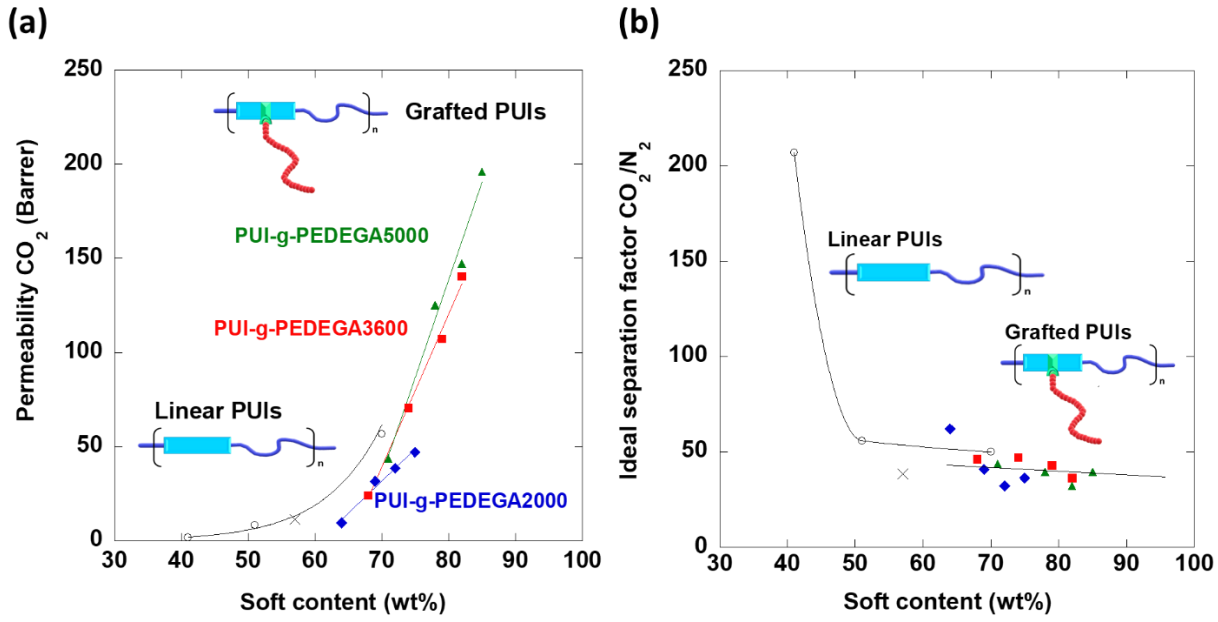

Fig. 9. Influence of copolymer soft content on (a) permeability of CO_2 and (b) ideal separation factor $\alpha CO_2/N_2$ for the grafted PUI copolymers (filled symbols), the precursor PUI-g (×) and the corresponding linear PUI copolymers (empty circle symbols, data taken from our former work [76]) at 2 bar and 35°C.

514

515 **Table 3. Membrane separation properties of the grafted PUI copolymers compared with different linear multi-block**
516 **copolymers with polyether soft blocks and their blends with PEO-based additives reported in the literature.**

Sample	P_{CO2} (Barrer)	$\alpha CO_2/N_2$	CO_2 pressure	T (°C)	Ref.
POLY(ETHER-AMIDE)S (PEBAX)					
Pebax 2533 (PTMO/PA12)	260	32	6.8 atm	25°C	[33]
Pebax 4033 (PTMO/PA12)	113	20	10 bar	35°C	[38]
Pebax 1074 (PEO-PA12)	133	43	2 bar	35°C	[46]
Pebax 1074 (PEO-PA12)	168	55	13.8 bar	35°C	[119]
Pebax 4011 (PEO/PA6)	66	56	10 atm	35°C	[38]
Pebax 1657 (PEO/PA6)	79	53	1 bar	30°C	[35]
Pebax 1657 (PEO/PA6)	157	47	3 bar	45°C	[45]
Pebax 1657 (PEO/PA6)	147	89	13.8 bar	35°C	[119]
POLY(ETHER-ESTER)S					
PEO-PBT	115	46	300 mbar	30°C	[30]
PEO-PTT	183	51	300 mbar	30°C	[31]
PEO_{2000}-T6T6T	180	49	4 atm	35°C	[43]
(PEO-*ran*-PPO)$_{2500}$-T6T6T	348	45	4 bar	35°C	[41]
Polyactive 1500 (PEGT/PBT)	226	37.7	1 bar	40°C	[34]
Polyactive 3000 (PEGT/PBT)	190	38	1 bar	40°C	[34]
Polyactive 4000 (PEGT/PBT)	75	37.5	1 bar	40°C	[34]
POLY(ETHER-URETHANE)S					
PU (PEO_{1000}/MDI/BD)	36	22	1 bar	30°C	[120]
PU (PEO_{2000}/MDI/BPA)	48	47	2 atm	35°C	[99]
PU (PEO-PU epoxy network)	63.4	57.6	2 bar	35°C	[55]
PU Ellastollan	41	68.2	1 bar	25°C	[53]
PU (PTMO/IPDI/BDA)	109	21.9	4 bar	30°C	[54]
PU (PTMO/HDI/Naphtyl-based diamine)	247	33.8	4 bar	30°C	[54]
POLY(ETHER-IMIDE)S					
PI (6FDA/JFAED600/6FpDA)	97	19	2 bar	25°C	[63]
PI (BPDA/JFAED2000/ODA)	60	50	3 bar	30°C	[61]
PI (ODPA/JFAED2003/ODA)	52	63	6 bar	30°C	[70]
PI (PMDA/JAFED2300/m-PD)	99	50	2 atm	35°C	[99]
PI (PMDA/PEO_{2000}/ODA)	10	60	3 bar	30°C	[62]
PI (BPDA/PEO_{6000}/ODA)	41	102	3 bar	30°C	[69]
PI (pent-PI-PEO_{2000})	39	46	3 atm	35°C	[65]
POLY(ETHER-UREA-IMIDE)S					
PUI JFAED600	2	207	2 bar	35°C	[76]
PUI JFAED900	8	56	2 bar	35°C	[76]
PUI JFAED2000	57	50	2 bar	35°C	[76]
Precursor PUI	11.5	38	2 bar	35°C	This work
PUI-g-1PEDEGA2000	47	36	2 bar	35°C	This work
PUI-g-1PEDEGA3600	140	36	2 bar	35°C	This work
PUI-g-1PEDEGA5000	196	39	2 bar	35°C	This work
RELATED MULTI-BLOCK					

COPOLYMER BLENDS WITH PEO-BASED ADDITIVES					
Pebax 1657/PEG200 (50wt%)	151	47	600 mbar	30°C	[121]
Pebax 1657/PEG200 (50wt%)	172	50.5	4 bar	35°C	[122]
Pebax 1657/PEG600 (40wt%)	62.9	83.8	3 bar	25°C	[123]
Pebax 1657/PEG-DME (50wt%)	606	43	300 mbar	30°C	[124]
Pebax 1657/PEG-DME (40wt%)	378	48	800 mbar	30°C	[35]
Pebax 1657/PEO-based polysorbate T20 (50 wt%)	144	50.7	1 bar	25°C	[125]
Pebax 1657/PEO-based polysorbate T80 (50 wt%)	167	47.8	1 bar	25°C	[125]
Pebax 1657/PDMS-PEG (50wt%)	532	36.1	4 bar	35°C	[122]
Pebax 1657/Crosslinked PEG-diacrylate	27.5	195.8	3 bar	25°C	[126]
Polyactive 1500/PEG-POSS (30 wt%)	334	37.1	1 bar	40°C	[34]
Pebax 1657/PEG550 (30wt%)/calix[4]arene(0.5 wt%)i	632.6	140	10 bar	35°C	[127]
Pebax 1657/PEG200 (20 wt%)/glycerol (15 wt%)/$NiFe_2O_4$ (3 wt%)	269	273.4	10 bar	35°C	[128]
Pebax 1657/PEG400 (1.5 wt%)/Porous organic polymer (1 wt%)	392	112	1 bar	30°C	[129]
Pebax 1657/PEG600 (20 wt%)/NaY (30 wt%)	172.6	107.9	1.5 bar	30°C	[130]

Table 3 makes a comparison of the membrane properties of the new grafted multi-block copolymers with other PEO (or PTMO)-based (linear/ungrafted) multi-block copolymers reported in literature for CO_2 capture. For experimental conditions close to those used in this work (feed pressure of 2 bar and temperature of 35°C), the best grafted PUI multi-block copolymer (PUI-g-1PEDEGA5000) offers high permeability (196 Barrer) and high selectivity (39) and ranks among the most permeable PEO-based multi-block copolymers with high selectivity $\alpha CO_2/N_2$ such as Pebax 1657 [35,45] and Polyactive 1500 [30,34]. However, as expected from the data reported in literature, PUI-g-1PEDEGA5000 does not compete with most of the multi-block copolymer blends with PEO-based additives, most of them having better CO_2 permeability or/and selectivity for CO_2 capture [35,45,121–126]. Nevertheless, PUI-g-1PEDEGA5000 could be an excellent candidate for new polymer blends with PEO-based additives or their combination with porous organic polymers, metal organic frameworks or metal oxides reported for this application [127–130]. The corresponding permeability-selectivity diagram (Fig. 10) refines this comparison and further illustrates the strong differences between the linear and grafted PUI multi-block copolymers. In addition to maintaining high selectivity for CO_2/N_2 separation, the grafted multi-block copolymers enabled a strong increase in CO_2 permeability going very close to the Robeson 2008 upper-bound for the separation of CO_2 from N_2.

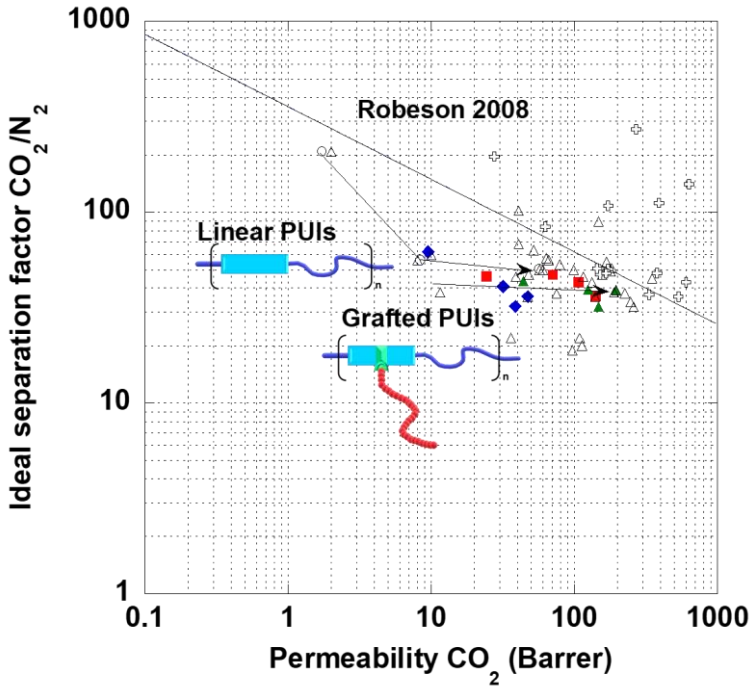

Fig. 10. Robeson plot showing the CO_2 separation performances of the grafted PUI copolymers (filled symbols), the corresponding linear PUI copolymers (empty circle symbols, data taken from our former work [76]**),different other linear polyether-based multi-block copolymers (empty triangles) and their blends with PEO-based additives (empty crosses) reported in the literature.**

4. Conclusion

A new strategic way of grafting was developed for PEO-based multi-block copolymers to improve their membrane performance for CO_2 capture. The grafted PUI multi-block copolymers were synthesized by combining step-growth polycondensation, controlled radical polymerization and "click" chemistry to provide good control of their structural parameters (grafting rate, number and length of the grafts, and copolymer soft content). The new grafting strategy allowed to strongly increase the copolymer soft content up to 85 wt% compared to the maximum soft content (ca. 70 wt%) obtained for the corresponding linear PUI copolymers reported in our former work [76].

The new grafted PUI multi-block copolymers were non-crystalline (amorphous) materials even for the highest copolymer soft contents. Since crystallinity is one of the most widespread limitations of PEO-based copolymers for CO_2 separation membranes, the grafted PUI materials were particularly suitable for this application. The physical cross-linking provided by their UI hard blocks allowed the obtaining of cohesive membrane materials with exceptionally high soft contents. Furthermore, by a strategic grafting of the PEO-based grafts onto specific hard blocks, the grafted multi-block copolymers displayed special nano-structuration and morphology, combining high to very high soft content and the dragging of the grafted hard blocks within the soft phase.

The CO_2 permeability strongly increased up to 17-fold with the grafting rate, graft molecular weight and copolymer soft content while the ideal separation factor $\alpha CO_2/N_2$ remained quasi-constant at a high level close to 40. The behavior of the grafted PUI copolymers was very different from that obtained for the corresponding linear PUI copolymers, which were strongly penalized by a permeability/selectivity trade-off in our former work. The particular behavior of the new grafted

copolymers was related to their special morphology involving impermeable obstacles dispersed in the highly permeable phase, allowing maintaining high membrane selectivity even for the highest soft contents.

The best membrane properties (196 Barrer and ideal separation factor of 39 at 2 Bar and 35°C) were finally obtained for PUI-g-1PEDEGA5000 combining the highest grafting rate (100%), the highest PEDEGA graft molecular weight (5000) and resulting copolymer soft content (85 wt%). A comparison with literature shows that this grafted copolymer ranks among the best PEO-based copolymers reported for CO_2/N_2 separation. This grafted copolymer shows a good permeability/selectivity compromise associated with a combination of good film-forming and adhesion properties onto different substrates. In the future, it could be used for developing mixed matrix membranes, thin layer composite membranes or blend membranes for CO_2 capture. Furthermore, the new grafting strategy could also be extended for designing a wide range of new high-performance membrane materials for CO_2 separations.

Supporting Information reports a figure showing an example of grafting monitoring by SEC-MALLS, a figure showing SEM pictures for membrane surfaces and cross-sections for precursor PUI-g and a grafted multi-block copolymer and a table reporting the permeability, sorption and diffusion coefficients for pure gases CO_2 and N_2 for the grafted PUI copolymers and their precursor PUI-g.

Acknowledgment: The results reported in this work and preliminary results on related mixed-matrix membranes enabled to obtain financial support from the CNRS for a new 2-year research project New Materials through the MITI interdisciplinary programs. The authors thank the Higher Education and Research French Ministry (MESR) for the PhD funding for Xavier Solimando.

5. References

[1] T.C. Merkel, H. Lin, X. Wei, R. Baker, Power plant post-combustion carbon dioxide capture: An opportunity for membranes, J. Membr. Sci. 359 (2010) 126–139. https://doi.org/10.1016/j.memsci.2009.10.041.

[2] C.E. Powell, G.G. Qiao, Polymeric CO2/N2 gas separation membranes for the capture of carbon dioxide from power plant flue gases, J. Membr. Sci. 279 (2006) 1–49. https://doi.org/10.1016/j.memsci.2005.12.062.

[3] H. Lin, Z. He, Z. Sun, J. Vu, A. Ng, M. Mohammed, J. Kniep, T.C. Merkel, T. Wu, R.C. Lambrecht, CO2-selective membranes for hydrogen production and CO2 capture – Part I: Membrane development, J. Membr. Sci. 457 (2014) 149–161. https://doi.org/10.1016/j.memsci.2014.01.020.

[4] E. Kintisch, The Greening of Synfuels, Science. 320 (2008) 306–308. https://doi.org/10.1126/science.320.5874.306.

[5] S. Sridhar, R. Suryamurali, B. Smitha, T.M. Aminabhavi, Development of crosslinked poly(ether-block-amide) membrane for CO2/CH4 separation, Colloids Surf A. 297 (2007) 267–274. https://doi.org/10.1016/j.colsurfa.2006.10.054.

[6] S. Sridhar, B. Smitha, T.M. Aminabhavi, Separation of Carbon Dioxide from Natural Gas Mixtures through Polymeric Membranes—A Review, Sep. Purif. Rev. 36 (2007) 113–174. https://doi.org/10.1080/15422110601165967.

[7] X. Hu, J. Tang, A. Blasig, Y. Shen, M. Radosz, CO2 permeability, diffusivity and solubility in polyethylene glycol-grafted polyionic membranes and their CO2 selectivity relative to methane and nitrogen, J. Membr. Sci. 281 (2006) 130–138. https://doi.org/10.1016/j.memsci.2006.03.030.

[8] A. Brunetti, F. Scura, G. Barbieri, E. Drioli, Membrane technologies for CO2 separation, J. Membr. Sci. 359 (2010) 115–125. https://doi.org/10.1016/j.memsci.2009.11.040.

[9] J.D. Figueroa, T. Fout, S. Plasynski, H. McIlvried, R.D. Srivastava, Advances in CO2 capture technology—The U.S. Department of Energy's Carbon Sequestration Program, Int. J. Greenh. Gas Control. 2 (2008) 9–20. https://doi.org/10.1016/S1750-5836(07)00094-1.

[10] U. Singh, Carbon capture and storage: an effective way to mitigate global warming, Curr. Sci. 105 (2013) 914–922. No DOI found for this reference.

[11] H.H. Khoo, R.B.H. Tan, Life Cycle Investigation of CO2 Recovery and Sequestration, Environ. Sci. Technol. 40 (2006) 4016–4024. https://doi.org/10.1021/es051882a.

[12] J. Liu, X. Hou, H.B. Park, H. Lin, High-Performance Polymers for Membrane CO2 /N2 Separation, Chem. Weinh. Bergstr. Ger. (2016). https://doi.org/10.1002/chem.201603002.

[13] M. Rezakazemi, A. Ebadi Amooghin, M.M. Montazer-Rahmati, A.F. Ismail, T. Matsuura, State-of-the-art membrane based CO2 separation using mixed matrix membranes (MMMs): An overview on current status and future directions, Prog. Polym. Sci. 39 (2014) 817–861. https://doi.org/10.1016/j.progpolymsci.2014.01.003.

[14] B. Seoane, J. Coronas, I. Gascon, M.E. Benavides, O. Karvan, J. Caro, F. Kapteijn, J. Gascon, Metal–organic framework based mixed matrix membranes: a solution for highly efficient CO2 capture?, Chem. Soc. Rev. 44 (2015) 2421–2454. https://doi.org/10.1039/C4CS00437J.

[15] S. Wang, X. Li, H. Wu, Z. Tian, Q. Xin, G. He, D. Peng, S. Chen, Y. Yin, Z. Jiang, M.D. Guiver, Advances in high permeability polymer-based membrane materials for CO_2 separations, Energy Environ. Sci. 9 (2016) 1863–1890. https://doi.org/10.1039/C6EE00811A.

[16] M. Ahmadi, S. Janakiram, Z. Dai, L. Ansaloni, L. Deng, Performance of Mixed Matrix Membranes Containing Porous Two-Dimensional (2D) and Three-Dimensional (3D) Fillers for CO2 Separation: A Review, Membranes. 8 (2018) 50. https://doi.org/10.3390/membranes8030050.

[17] A. Kargari, S. Rezaeinia, State-of-the-art modification of polymeric membranes by PEO and PEG for carbon dioxide separation: A review of the current status and future perspectives, J. Ind. Eng. Chem. 84 (2020) 1–22. https://doi.org/10.1016/j.jiec.2019.12.020.

[18] M. Kárászová, B. Zach, Z. Petrusová, V. Červenka, M. Bobák, M. Šyc, P. Izák, Post-combustion carbon capture by membrane separation, Review, Sep. Purif. Technol. 238 (2020) 116448. https://doi.org/10.1016/j.seppur.2019.116448.
[19] A.S. Embaye, L. Martínez-Izquierdo, M. Malankowska, C. Téllez, J. Coronas, Poly(ether- *block* -amide) Copolymer Membranes in CO_2 Separation Applications, Energy Fuels. 35 (2021) 17085–17102. https://doi.org/10.1021/acs.energyfuels.1c01638.
[20] S. Bandehali, A. Moghadassi, F. Parvizian, S.M. Hosseini, T. Matsuura, E. Joudaki, Advances in high carbon dioxide separation performance of poly (ethylene oxide)-based membranes, J. Energy Chem. 46 (2020) 30–52. https://doi.org/10.1016/j.jechem.2019.10.019.
[21] S.R. Reijerkerk, M. Wessling, K. Nijmeijer, Pushing the limits of block copolymer membranes for CO2 separation, J. Membr. Sci. 378 (2011) 479–484. https://doi.org/10.1016/j.memsci.2011.05.039.
[22] L. Dong, Y. Wang, M. Chen, D. Shi, X. Li, C. Zhang, H. Wang, Enhanced CO2 separation performance of P(PEGMA-co-DEAEMA-co-MMA) copolymer membrane through the synergistic effect of EO groups and amino groups, RSC Adv. 6 (2016) 59946–59955. https://doi.org/10.1039/C6RA10475D.
[23] J.H. Lee, J.P. Jung, E. Jang, K.B. Lee, Y.S. Kang, J.H. Kim, CO2-philic PBEM-g-POEM comb copolymer membranes: Synthesis, characterization and CO2/N2 separation, J. Membr. Sci. 502 (2016) 191–201. https://doi.org/10.1016/j.memsci.2015.12.005.
[24] H. Lin, B.D. Freeman, Gas and Vapor Solubility in Cross-Linked Poly(ethylene Glycol Diacrylate), Macromolecules. 38 (2005) 8394–8407. https://doi.org/10.1021/ma051218e.
[25] A. Ghadimi, S. Norouzbahari, V. Vatanpour, F. Mohammadi, An Investigation on Gas Transport Properties of Cross-Linked Poly(ethylene glycol diacrylate) (XLPEGDA) and XLPEGDA/TiO_2 Membranes with a Focus on CO_2 Separation, Energy Fuels. 32 (2018) 5418–5432. https://doi.org/10.1021/acs.energyfuels.8b00545.
[26] F.H. Akhtar, M. Kumar, H. Vovusha, R. Shevate, L.F. Villalobos, U. Schwingenschlögl, K.-V. Peinemann, Scalable Synthesis of Amphiphilic Copolymers for CO_2 - and Water-Selective Membranes: Effect of Copolymer Composition and Chain Length, Macromolecules. 52 (2019) 6213–6226. https://doi.org/10.1021/acs.macromol.9b00528.
[27] S.J. Metz, M.H.V. Mulder, M. Wessling, Gas-Permeation Properties of Poly(ethylene oxide) Poly(butylene terephthalate) Block Copolymers, Macromolecules. 37 (2004) 4590–4597. https://doi.org/10.1021/ma049847w.
[28] S.J. Metz, J. Potreck, M.H.V. Mulder, M. Wessling, Water vapor and gas transport through a poly(butylene terephthalate) poly(ethylene oxide) block copolymer, Desalination. 148 (2002) 303–307. https://doi.org/10.1016/S0011-9164(02)00721-X.
[29] S.J. Metz, W.J.C. van de Ven, J. Potreck, M.H.V. Mulder, M. Wessling, Transport of water vapor and inert gas mixtures through highly selective and highly permeable polymer membranes, J. Membr. Sci. 251 (2005) 29–41. https://doi.org/10.1016/j.memsci.2004.08.036.
[30] A. Car, C. Stropnik, W. Yave, K.-V. Peinemann, Tailor-made Polymeric Membranes based on Segmented Block Copolymers for CO2 Separation, Adv. Funct. Mater. 18 (2008) 2815–2823. https://doi.org/10.1002/adfm.200800436.
[31] W. Yave, A. Szymczyk, N. Yave, Z. Roslaniec, Design, synthesis, characterization and optimization of PTT-b-PEO copolymers: A new membrane material for CO2 separation, J. Membr. Sci. 362 (2010) 407–416. https://doi.org/10.1016/j.memsci.2010.06.060
[32] J. Liu, X. Hou, H.B. Park, H. Lin, High-Performance Polymers for Membrane CO2 /N2 Separation, Chem. Weinh. Bergstr. Ger. (2016). https://doi.org/10.1002/chem.201603002.
[33] S.L. Liu, L. Shao, M.L. Chua, C.H. Lau, H. Wang, S. Quan, Recent progress in the design of advanced PEO-containing membranes for CO2 removal, Prog. Polym. Sci. 38 (2013) 1089–1120. https://doi.org/10.1016/j.progpolymsci.2013.02.002.
[34] Md.M. Rahman, V. Filiz, S. Shishatskiy, C. Abetz, P. Georgopanos, M.M. Khan, S. Neumann, V. Abetz, Influence of Poly(ethylene glycol) Segment Length on CO_2 Permeation and Stability of

PolyActive Membranes and Their Nanocomposites with PEG POSS, ACS Appl. Mater. Interfaces. 7 (2015) 12289–12298. https://doi.org/10.1021/am504223f.
[35] J. Lillepärg, P. Georgopanos, S. Shishatskiy, Stability of blended polymeric materials for CO2 separation, J. Membr. Sci. 467 (2014) 269–278. https://doi.org/10.1016/j.memsci.2014.05.039.
[36] J. Lillepärg, E. Sperling, M. Blanke, M. Held, S. Shishatskiy, Multicomponent Network Formation in Selective Layer of Composite Membrane for CO2 Separation, Membranes. 11 (2021) 174. https://doi.org/10.3390/membranes11030174.
[37] Md.M. Rahman, J. Lillepärg, S. Neumann, S. Shishatskiy, V. Abetz, A thermodynamic study of CO2 sorption and thermal transition of PolyActive™ under elevated pressure, Polymer. 93 (2016) 132–141. https://doi.org/10.1016/j.polymer.2016.04.024.
[38] V.I. Bondar, B.D. Freeman, I. Pinnau, Gas transport properties of poly(ether-b-amide) segmented block copolymers, J. Polym. Sci. Part B Polym. Phys. 38 (2000) 2051–2062. https://doi.org/10.1002/1099-0488(20000801)38:15<2051::AID-POLB100>3.0.CO;2-D.
[39] V.I. Bondar, B.D. Freeman, I. Pinnau, Gas sorption and characterization of poly(ether-b-amide) segmented block copolymers, J. Polym. Sci. Part B Polym. Phys. 37 (1999) 2463–2475. https://doi.org/10.1002/(SICI)1099-0488(19990901)37:17<2463::AID-POLB18>3.0.CO;2-H.
[40] S.R. Reijerkerk, A. Arun, R.J. Gaymans, K. Nijmeijer, M. Wessling, Tuning of mass transport properties of multi-block copolymers for CO2 capture applications, J. Membr. Sci. 359 (2010) 54–63. https://doi.org/10.1016/j.memsci.2009.09.045.
[41] S.R. Reijerkerk, A.C. Ijzer, K. Nijmeijer, A. Arun, R.J. Gaymans, M. Wessling, Subambient Temperature CO2 and Light Gas Permeation Through Segmented Block Copolymers with Tailored Soft Phase, ACS Appl. Mater. Interfaces. 2 (2010) 551–560. https://doi.org/10.1021/am900754z.
[42] A.C. IJzer, A. Arun, S.R. Reijerkerk, K. Nijmeijer, M. Wessling, R.J. Gaymans, Synthesis and properties of hydrophilic segmented block copolymers based on poly(ethylene oxide)-ran-poly(propylene oxide), J. Appl. Polym. Sci. 117 (2010) 1394–1404. https://doi.org/10.1002/app.31906.
[43] D. Husken, T. Visser, M. Wessling, R.J. Gaymans, CO2 permeation properties of poly(ethylene oxide)-based segmented block copolymers, J. Membr. Sci. 346 (2010) 194–201. https://doi.org/10.1016/j.memsci.2009.09.034.
[44] K. Kim, P.G. Ingole, J. Kim, H. Lee, Separation performance of PEBAX/PEI hollow fiber composite membrane for SO2/CO2/N2 mixed gas, Chem. Eng. J. 233 (2013) 242–250. https://doi.org/10.1016/j.cej.2013.08.030.
[45] J.H. Kim, S.Y. Ha, Y.M. Lee, Gas permeation of poly(amide-6-b-ethylene oxide) copolymer, J. Membr. Sci. 190 (2001) 179–193. https://doi.org/10.1016/S0376-7388(01)00444-6.
[46] X. Solimando, C. Lherbier, J. Babin, C. Arnal-Herault, E. Romero, S. Acherar, B. Jamart-Gregoire, D. Barth, D. Roizard, A. Jonquieres, Pseudopeptide bioconjugate additives for CO2 separation membranes, Polym. Int. 65 (2016) 1464–1473. https://doi.org/10.1002/pi.5240.
[47] H. Rabiee, S. Meshkat Alsadat, M. Soltanieh, S.A. Mousavi, A. Ghadimi, Gas permeation and sorption properties of poly(amide-12-b-ethyleneoxide)(Pebax1074)/SAPO-34 mixed matrix membrane for CO2/CH4 and CO2/N2 separation, J. Ind. Eng. Chem. 27 (2015) 223–239. https://doi.org/10.1016/j.jiec.2014.12.039.
[48] V. Barbi, S.S. Funari, R. Gehrke, N. Scharnagl, N. Stribeck, SAXS and the Gas Transport in Polyether-block-polyamide Copolymer Membranes, Macromolecules. 36 (2003) 749–758. https://doi.org/10.1021/ma0213403.
[49] T. Préfol, O. Gain, G. Sudre, F. Gouanvé, E. Espuche, Development of Breathable Pebax®/PEG Films for Optimization of the Shelf-Life of Fresh Agri-Food Products, Membranes. 11 (2021) 692. https://doi.org/10.3390/membranes11090692.
[50] A.P. Isfahani, B. Ghalei, R. Bagheri, Y. Kinoshita, H. Kitagawa, E. Sivaniah, M. Sadeghi, Polyurethane gas separation membranes with ethereal bonds in the hard segments, J. Membr. Sci. 513 (2016) 58–66. https://doi.org/10.1016/j.memsci.2016.04.030.

[51] L.-S. Teo, J.-F. Kuo, C.-Y. Chen, Study on the morphology and permeation property of amine group-contained polyurethanes, Polymer. 39 (1998) 3355–3364. https://doi.org/10.1016/S0032-3861(97)10090-8.
[52] A. Pournaghshband Isfahani, M. Sadeghi, K. Wakimoto, B.B. Shrestha, R. Bagheri, E. Sivaniah, B. Ghalei, Pentiptycene-Based Polyurethane with Enhanced Mechanical Properties and CO_2-Plasticization Resistance for Thin Film Gas Separation Membranes, ACS Appl. Mater. Interfaces. 10 (2018) 17366–17374. https://doi.org/10.1021/acsami.7b18475.
[53] C.D. García Jiménez, A.C. Habert, C.P. Borges, Polyurethane/polyethersulfone dual-layer anisotropic membranes for CO_2 removal from flue gas, J. Appl. Polym. Sci. 138 (2021) 50476. https://doi.org/10.1002/app.50476.
[54] A. Fakhar, M. Sadeghi, M. Dinari, R. Lammertink, Association of hard segments in gas separation through polyurethane membranes with aromatic bulky chain extenders, J. Membr. Sci. 574 (2019) 136–146. https://doi.org/10.1016/j.memsci.2018.12.062.
[55] S. Norouzbahari, R. Gharibi, An investigation on structural and gas transport properties of modified cross-linked PEG-PU membranes for CO2 separation, React. Funct. Polym. 151 (2020) 104585. https://doi.org/10.1016/j.reactfunctpolym.2020.104585.
[56] R. Gharibi, A. Ghadimi, H. Yeganeh, B. Sadatnia, M. Gharedaghi, Preparation and evaluation of hybrid organic-inorganic poly(urethane-siloxane) membranes with build-in poly(ethylene glycol) segments for efficient separation of CO2/CH4 and CO2/H2, J. Membr. Sci. 548 (2018) 572–582. https://doi.org/10.1016/j.memsci.2017.11.058.
[57] L.-S. Teo, J.-F. Kuo, C.-Y. Chen, Permeation and sorption of CO2 through amine-contained polyurethane and poly(urea–urethane) membranes, J. Appl. Polym. Sci. 59 (1996) 1627–1638. https://doi.org/10.1002/(SICI)1097-4628(19960307)59:10<1627::AID-APP15>3.0.CO;2-T.
[58] L. Olivieri, A. Tena, M.G. De Angelis, A.H. Giménez, A.E. Lozano, G.C. Sarti, Sorption and transport of CO2 in copolymers containing soft (PEO, PPO) and hard (BKDA-ODA and BPDA-ODA) segments at different temperatures: Experimental data and modeling, J. Membr. Sci. 520 (2016) 187–200. https://doi.org/10.1016/j.memsci.2016.07.057.
[59] A. Tena, A. Marcos-Fernández, A.E. Lozano, J.G. de la Campa, J. de Abajo, L. Palacio, P. Prádanos, A. Hernández, Thermally treated copoly(ether-imide)s made from bpda and alifatic plus aromatic diamines. Gas separation properties with different aromatic diamimes, J. Membr. Sci. 387–388 (2012) 54–65. https://doi.org/10.1016/j.memsci.2011.10.008.
[60] D.M. Munoz, E.M. Maya, J. de Abajo, Thermal treatment of poly (ethylene oxide)-segmented copolyimide based membranes: An effective way to improve the gas separation properties, J. Membr. Sci. 323 (2008) 53–59. https://doi.org/10.1016/j.memsci.2008.06.036.
[61] A. Tena, A. Marcos-Fernández, L. Palacio, P. Prádanos, A.E. Lozano, J. de Abajo, A. Hernández, On the influence of the proportion of PEO in thermally controlled phase segregation of copoly(ether-imide)s for gas separation, J. Membr. Sci. 434 (2013) 26–34. https://doi.org/10.1016/j.memsci.2013.01.036.
[62] A. Tena, Á. Marcos-Fernández, M. de la Viuda, L. Palacio, P. Prádanos, Á.E. Lozano, J. de Abajo, A. Hernández, Advances in the design of co-poly(ether-imide) membranes for CO2 separations. Influence of aromatic rigidity on crystallinity, phase segregation and gas transport, Eur. Polym. J. 62 (2015) 130–138. https://doi.org/10.1016/j.eurpolymj.2014.11.016.
[63] M. Krea, D. Roizard, E. Favre, Copoly(Alkyl ether imide) membranes as promising candidates for CO2 capture applications, Sep. Purif. Technol. 161 (2016) 53–60. https://doi.org/10.1016/j.seppur.2016.01.045.
[64] M. Khoshkam, M. Sadeghi, M.P. Chenar, M. Naghsh, M.J.N. Fard, M. Shafiei, Synthesis, characterization and gas separation properties of novel copolyimide membranes based on flexible etheric–aliphatic moieties, RSC Adv. 6 (2016) 35751–35763. https://doi.org/10.1039/C6RA04973G.
[65] S. Luo, K.A. Stevens, J.S. Park, J.D. Moon, Q. Liu, B.D. Freeman, R. Guo, Highly CO2-Selective Gas Separation Membranes Based on Segmented Copolymers of Poly(Ethylene oxide) Reinforced

with Pentiptycene-Containing Polyimide Hard Segments, ACS Appl. Mater. Interfaces. 8 (2016) 2306–2317. https://doi.org/10.1021/acsami.5b11355.
[66] H. Chen, Y. Xiao, T.-S. Chung, Synthesis and characterization of poly (ethylene oxide) containing copolyimides for hydrogen purification, Polymer. 51 (2010) 4077–4086. https://doi.org/10.1016/j.polymer.2010.06.046.
[67] M. Askari, M.L. Chua, T.-S. Chung, Permeability, Solubility, Diffusivity, and PALS Data of Cross-linkable 6FDA-based Copolyimides, Ind. Eng. Chem. Res. 53 (2014) 2449–2460. https://doi.org/10.1021/ie403505u.
[68] M. Askari, Y. Xiao, P. Li, T.-S. Chung, Natural gas purification and olefin/paraffin separation using cross-linkable 6FDA-Durene/DABA co-polyimides grafted with α, β, and γ-cyclodextrin, J. Membr. Sci. 390–391 (2012) 141–151. https://doi.org/10.1016/j.memsci.2011.11.030.
[69] A. Marcos-Fernández, E. Adem, A.R. Hernández-Sampelayo, J.E. Báez, L. Palacio, P. Prádanos, A. Tena, A. Hernández, Elimination of the Crystallinity of Long Polyethylene Oxide-Based Copolymers for Gas Separation Membranes by Using Electron Beam Irradiation, Macromol. Chem. Phys. 218 (2017) 1600441. https://doi.org/10.1002/macp.201600441.
[70] A. Jankowski, E. Grabiec, K. Nocoń-Szmajda, A. Marcinkowski, H. Janeczek, A. Wolińska-Grabczyk, Polyimide-Based Membrane Materials for CO2 Separation: A Comparison of Segmented and Aromatic (Co)polyimides, Membranes. 11 (2021) 274. https://doi.org/10.3390/membranes11040274.
[71] H. Sanaeepur, A. Ebadi Amooghin, S. Bandehali, A. Moghadassi, T. Matsuura, B. Van der Bruggen, Polyimides in membrane gas separation: Monomer's molecular design and structural engineering, Prog. Polym. Sci. 91 (2019) 80–125. https://doi.org/10.1016/j.progpolymsci.2019.02.001.
[72] Y. Xiao, B.T. Low, S.S. Hosseini, T.S. Chung, D.R. Paul, The strategies of molecular architecture and modification of polyimide-based membranes for CO2 removal from natural gas-A review, Prog. Polym. Sci. 34 (2009) 561–580. https://doi.org/10.1016/j.progpolymsci.2008.12.004.
[73] L. Jujie, X. He, Z. Si, Polysulfone membranes containing ethylene glycol monomers: synthesis, characterization, and CO2/CH4 separation, J. Polym. Res. 24 (2016) 1. https://doi.org/10.1007/s10965-016-1163-6.
[74] H.W. Kim, H.B. Park, Gas diffusivity, solubility and permeability in polysulfone–poly(ethylene oxide) random copolymer membranes, J. Membr. Sci. 372 (2011) 116–124. https://doi.org/10.1016/j.memsci.2011.01.053.
[75] A. Car, C. Stropnik, W. Yave, K.-V. Peinemann, Pebax (R)/Polyethylene glycol blend thin film composite membranes for CO2 separation: Performance with mixed gases, Sep. Purif. Technol. 62 (2008) 110–117. https://doi.org/10.1016/j.seppur.2008.01.001.
[76] X. Solimando, J. Babin, C. Arnal-Herault, M. Wang, D. Barth, D. Roizard, J.-R. Doillon-Halmenschlager, M. Ponçot, I. Royaud, P. Alcouffe, L. David, A. Jonquieres, Highly selective multi-block poly(ether-urea-imide)s for CO2/N2 separation: Structure-morphology-properties relationships, Polymer. 131 (2017) 56–67. https://doi.org/10.1016/j.polymer.2017.10.007.
[77] S.H. Ahn, J.A. Seo, J.H. Kim, Y. Ko, S.U. Hong, Synthesis and gas permeation properties of amphiphilic graft copolymer membranes, J. Membr. Sci. 345 (2009) 128–133. https://doi.org/10.1016/j.memsci.2009.08.037.
[78] G.-L. Zhuang, M.-Y. Wey, H.-H. Tseng, A novel technique using reclaimed tire rubber for gas separation membranes, J. Membr. Sci. 520 (2016) 314–325. https://doi.org/10.1016/j.memsci.2016.07.044.
[79] Yu.V. Ivanova, G.A. Shandryuk, D. Roizard, D. Barth, V.S. Khotimskiy, Synthesis of polyvinyltrimethylsilane-graft-poly(ethylene glycol) copolymers and properties of gas-separating membranes formed on their basis, Polym. Sci. Ser. B. 56 (2014) 282–289. https://doi.org/10.1134/S1560090414030087.

[80] C.S. Lee, N.U. Kim, J.T. Park, J.H. Kim, Imidazole-functionalized hydrophilic rubbery comb copolymers: Microphase-separation and good gas separation properties, Sep. Purif. Technol. 242 (2020) 116780. https://doi.org/10.1016/j.seppur.2020.116780.
[81] D.H. Kim, M.S. Park, Y. Choi, K.B. Lee, J.H. Kim, Synthesis of PVA-g-POEM graft copolymers and their use in highly permeable thin film composite membranes, Chem. Eng. J. 346 (2018) 739–747. https://doi.org/10.1016/j.cej.2018.04.036.
[82] I. Taniguchi, K. Kinugasa, S. Egashira, M. Higa, Preparation of well-defined hyper-branched polymers and the CO2 separation performance, J. Membr. Sci. 502 (2016) 124–132. https://doi.org/10.1016/j.memsci.2015.12.032.
[83] I. Taniguchi, N. Wada, K. Kinugasa, M. Higa, A strategy to enhance CO2 permeability of well-defined hyper-branched polymers with dense polyoxyethylene comb graft, J. Membr. Sci. 535 (2017) 239–247. https://doi.org/10.1016/j.memsci.2017.04.046.
[84] S.J. Kim, H. Jeon, D.J. Kim, J.H. Kim, High-performance Polymer Membranes with Multi-functional Amphiphilic Micelles for CO_2 Capture, ChemSusChem. 8 (2015) 3731–3731. https://doi.org/10.1002/cssc.201501378.
[85] N.U. Kim, B.J. Park, J.H. Lee, J.H. Kim, High-performance ultrathin mixed-matrix membranes based on an adhesive PGMA- *co* -POEM comb-like copolymer for CO_2 capture, J. Mater. Chem. A. 7 (2019) 14723–14731. https://doi.org/10.1039/C9TA02962A.
[86] B.J. Park, N.U. Kim, C.S. Lee, J.H. Kim, Synthesis, Characterization, and CO2/N2 Separation Performance of POEM-g-PAcAm Comb Copolymer Membranes, Polymers. 13 (2021) 177. https://doi.org/10.3390/polym13020177.
[87] M.S. Park, N.U. Kim, B.J. Park, D.Y. Ryu, J.H. Kim, Ultra-selective ferric ion-complexed membranes composed of water-based zwitterionic comb copolymers, J. Mater. Chem. A. 7 (2019) 20847–20853. https://doi.org/10.1039/C9TA06216E.
[88] K. Kim, D.A. Kang, J.T. Park, K.C. Kim, J.H. Kim, Synthesis, structure and gas separation properties of ethanol-soluble, amphiphilic POM-PBHP comb copolymers, Polymer. 180 (2019) 121700. https://doi.org/10.1016/j.polymer.2019.121700.
[89] D.A. Kang, K. Kim, J.Y. Lim, J.T. Park, J.H. Kim, Mixed matrix membranes consisting of ZIF-8 in rubbery amphiphilic copolymer: Simultaneous improvement in permeability and selectivity, Chem. Eng. Res. Des. 153 (2020) 175–186. https://doi.org/10.1016/j.cherd.2019.10.009.
[90] D. Tian, T. Alebrahim, G.K. Kline, L. Chen, H. Lin, C. Bae, Structure and gas transport characteristics of triethylene oxide-grafted polystyrene- *b* -poly(ethylene- *co* -butylene)- *b* -polystyrene, J. Polym. Sci. 58 (2020) 2654–2663. https://doi.org/10.1002/pol.20200232.
[91] C.H. Park, J.H. Lee, J.P. Jung, W. Lee, D.Y. Ryu, J.H. Kim, Orientation of an Amphiphilic Copolymer to a Lamellar Structure on a Hydrophobic Surface and Implications for CO_2 Capture Membranes, Angew. Chem. Int. Ed. 58 (2019) 1143–1147. https://doi.org/10.1002/anie.201811450.
[92] T. Hong, P.-F. Cao, S. Zhao, B. Li, C. Smith, M. Lehmann, A.J. Erwin, S.M. Mahurin, S.R. Venna, A.P. Sokolov, T. Saito, Tailored CO_2 -philic Gas Separation Membranes via One-Pot Thiol–ene Chemistry, Macromolecules. 52 (2019) 5819–5828. https://doi.org/10.1021/acs.macromol.9b00497.
[93] J.P. Jung, C.H. Park, J.H. Lee, Y.-S. Bae, J.H. Kim, Room-temperature, one-pot process for CO2 capture membranes based on PEMA-g-PPG graft copolymer, Chem. Eng. J. 313 (2017) 1615–1622. https://doi.org/10.1016/j.cej.2016.11.031.
[94] Y. Yu, Y. Ma, J. Yin, C. Zhang, G. Feng, Y. Zhang, J. Meng, Tuning the micro-phase separation of the PES-g-PEG comb-like copolymer membrane for efficient CO2 separation, Sep. Purif. Technol. 265 (2021) 118465. https://doi.org/10.1016/j.seppur.2021.118465.
[95] J.H. Lee, H.T. Kwon, S. Bae, J. Kim, J.H. Kim, Mixed-matrix membranes containing nanocage-like hollow ZIF-8 polyhedral nanocrystals in graft copolymers for carbon dioxide/methane separation, Sep. Purif. Technol. 207 (2018) 427–434. https://doi.org/10.1016/j.seppur.2018.06.076.

[96] J.H. Lee, K. Im, S. Han, S.J. Yoo, J. Kim, J.H. Kim, Bimodal-porous hollow MgO sphere embedded mixed matrix membranes for CO2 capture, Sep. Purif. Technol. 250 (2020) 117065. https://doi.org/10.1016/j.seppur.2020.117065.
[97] I. Taniguchi, N. Wada, K. Kinugasa, M. Higa, CO_2 capture by polymeric membranes composed of hyper-branched polymers with dense poly(oxyethylene) comb and poly(amidoamine), Open Phys. 15 (2017) 662–670. https://doi.org/10.1515/phys-2017-0077.
[98] S. Luo, K.A. Stevens, J.S. Park, J.D. Moon, Q. Liu, B.D. Freeman, R. Guo, Highly CO2-Selective Gas Separation Membranes Based on Segmented Copolymers of Poly(Ethylene oxide) Reinforced with Pentiptycene-Containing Polyimide Hard Segments, ACS Appl. Mater. Interfaces. 8 (2016) 2306–2317. https://doi.org/10.1021/acsami.5b11355.
[99] M. Yoshino, K. Ito, H. Kita, K.-I. Okamoto, Effects of hard-segment polymers on CO2/N2 gas-separation properties of poly(ethylene oxide)-segmented copolymers, J. Polym. Sci. Part B Polym. Phys. 38 (2000) 1707–1715. https://doi.org/10.1002/1099-0488(20000701)38:13<1707::AID-POLB40>3.0.CO;2-W.
[100] B. Masiulanis, R. Zieliński, Mechanical, thermal, and electric properties of polyurethaneimide elastomers, J. Appl. Polym. Sci. 30 (1985) 2731–2741. https://doi.org/10.1002/app.1985.070300702.
[101] T. Takeichi, K. Ujiie, K. Inoue, High performance poly(urethane-imide) prepared by introducing imide blocks into the polyurethane backbone, Polymer. 46 (2005) 11225–11231. https://doi.org/10.1016/j.polymer.2005.09.075.
[102] M. Awkal, A. Jonquieres, R. Clement, P. Lochon, Synthesis and characterization of film-forming poly(urethaneimide) cationomers containing quaternary ammonium groups, Polymer. 47 (2006) 5724–5735. https://doi.org/10.1016/j.polymer.2006.05.058.
[103] M. Wang, C. Arnal-Herault, C. Rousseau, A. Palenzuela, J. Babin, L. David, A. Jonquieres, Grafting of multi-block copolymers: A new strategy for improving membrane separation performance for ethyl tert-butyl (ETBE) bio-fuel purification by pervaporation, J. Membr. Sci. 469 (2014) 31–42. https://doi.org/10.1016/j.memsci.2014.06.038.
[104] L.Q. Xu, F. Yao, G.-D. Fu, L. Shen, Simultaneous “Click Chemistry” and Atom Transfer Radical Emulsion Polymerization and Prepared Well-Defined Cross-Linked Nanoparticles, Macromolecules. 42 (2009) 6385–6392. https://doi.org/10.1021/ma901019r.
[105] S. Vijay Kumar, C. Arnal-Herault, M. Wang, J. Babin, A. Jonquieres, Multiblock Copolymer Grafting for Butanol Biofuel Recovery by a Sustainable Membrane Process, ACS Appl. Mater. Interfaces. 8 (2016) 16262–16272. https://doi.org/10.1021/acsami.6b01900.
[106] X. Solimando, C. Lherbier, J. Babin, C. Arnal-Herault, E. Romero, S. Acherar, B. Jamart-Gregoire, D. Barth, D. Roizard, A. Jonquieres, Pseudopeptide bioconjugate additives for CO2 separation membranes, Polym. Int. 65 (2016) 1464–1473. https://doi.org/10.1002/pi.5240.
[107] J.G. Wijmans, R.W. Baker, The solution-diffusion model: a review, J. Membr. Sci. 107 (1995) 1–21. https://doi.org/10.1016/0376-7388(95)00102-I.
[108] A. Jonquières, D. Roizard, J. Cuny, A. Vicherat, P. Lochon, Polarity measurements in block copolymers (polyurethaneimides) and correlation with their pervaporation features, J. Appl. Polym. Sci. 56 (1995) 1567–1579. https://doi.org/10.1002/app.1995.070561207.
[109] A. Sendijarević, V. Sendijarević, K.C. Frisch, B. Koruga-Lazarević, E. Torlić, Synthesis and properties of urethane-modified polyimides, J. Polym. Sci. Part Polym. Chem. 28 (1990) 3603–3615. https://doi.org/10.1002/pola.1990.080281307.
[110] T.-L. Wang, F.-J. Huang, Synthesis and properties of poly(amide-imide-urethane) thermoplastic elastomers, Polym. Int. 46 (1998) 280–284. https://doi.org/10.1002/(SICI)1097-0126(199808)46:4<280::AID-PI992>3.0.CO;2-#.
[111] J. Liu, D. Ma, Z. Li, FTIR studies on the compatibility of hard–soft segments for polyurethane–imide copolymers with different soft segments, Eur. Polym. J. 38 (2002) 661–665. https://doi.org/10.1016/S0014-3057(01)00247-6.

[112] H. Yeganeh, M.A. Shamekhi, Poly(urethane-imide-imide), a new generation of thermoplastic polyurethane elastomers with enhanced thermal stability, Polymer. 45 (2004) 359–365. https://doi.org/10.1016/j.polymer.2003.11.006.
[113] S. Mallakpour, F. Rafiemanzelat, Synthesis and characterization of new optically active poly(amide–imide–urethane) thermoplastic elastomers, derived from bis(p-amido benzoic acid)-N-trimellitylimido-l-leucine and polyoxyethylene-MDI, React. Funct. Polym. 62 (2005) 153–167. https://doi.org/10.1016/j.reactfunctpolym.2004.11.005.
[114] F. Qiu, D. Yang, G. Cao, R. Zhang, P. Li, Synthesis, characterization, thermal stability and thermo-optical properties of poly(urethane-imide), Sens. Actuators B-Chem. - Sens. Actuators B-Chem. 135 (2009) 449–454. https://doi.org/10.1016/j.snb.2008.10.040.
[115] I. Ben Youssef, H. Alem, F. Sarry, O. Elmazria, R. Jimenez Rioboo, C. Arnal-Hérault, A. Jonquières, Functional poly(urethane-imide)s containing Lewis bases for SO2 detection by Love surface acoustic wave gas micro-sensors, Sens. Actuators B Chem. 185 (2013) 309–320. https://doi.org/10.1016/j.snb.2013.04.120.
[116] H. Lin, B.D. Freeman, Materials selection guidelines for membranes that remove CO2 from gas mixtures, J. Mol. Struct. 739 (2005) 57–74. https://doi.org/10.1016/j.molstruc.2004.07.045.
[117] S.R. Reijerkerk, K. Nijmeijer, C.P. Ribeiro Jr., B.D. Freeman, M. Wessling, On the effects of plasticization in CO2/light gas separation using polymeric solubility selective membranes, J. Membr. Sci. 367 (2011) 33–44. https://doi.org/10.1016/j.memsci.2010.10.035.
[118] A. Jonquieres, R. Clément, P. Lochon, Permeability of block copolymers to vapors and liquids, Prog. Polym. Sci. 27 (2002) 1803–1877. https://doi.org/10.1016/S0079-6700(02)00024-2.
[119] Y. Wang, H. Li, G. Dong, C. Scholes, V. Chen, Effect of Fabrication and Operation Conditions on CO_2 Separation Performance of PEO–PA Block Copolymer Membranes, Ind. Eng. Chem. Res. 54 (2015) 7273–7283. https://doi.org/10.1021/acs.iecr.5b01234.
[120] H.B. Park, C.K. Kim, Y.M. Lee, Gas separation properties of polysiloxane/polyether mixed soft segment urethane urea membranes, J. Membr. Sci. 204 (2002) 257–269. https://doi.org/10.1016/S0376-7388(02)00048-0.
[121] A. Car, C. Stropnik, W. Yave, K.-V. Peinemann, PEG modified poly(amide-b-ethylene oxide) membranes for CO2 separation, J. Membr. Sci. 307 (2008) 88–95. https://doi.org/10.1016/j.memsci.2007.09.023.
[122] S.R. Reijerkerk, M.H. Knoef, K. Nijmeijer, M. Wessling, Poly(ethylene glycol) and poly(dimethyl siloxane): Combining their advantages into efficient CO2 gas separation membranes, J. Membr. Sci. 352 (2010) 126–135. https://doi.org/10.1016/j.memsci.2010.02.008.
[123] P. Taheri, A. Raisi, M.S. Maleh, CO2-selective poly (ether-block-amide)/polyethylene glycol composite blend membrane for CO2 separation from gas mixtures, Environ. Sci. Pollut. Res. 28 (2021) 38274–38291. https://doi.org/10.1007/s11356-021-13447-y.
[124] W. Yave, A. Car, K.-V. Peinemann, Nanostructured membrane material designed for carbon dioxide separation, J. Membr. Sci. 350 (2010) 124–129. https://doi.org/10.1016/j.memsci.2009.12.019.
[125] P. Bernardo, G. Clarizia, Enhancing Gas Permeation Properties of Pebax® 1657 Membranes via Polysorbate Nonionic Surfactants Doping, Polymers. 12 (2020) 253. https://doi.org/10.3390/polym12020253.
[126] P. Taheri, M.S. Maleh, A. Raisi, Cross-linking of poly (ether-block-amide) by poly (ethylene glycol) diacrylate to prepare plasticizing-resistant CO2-selective membranes, J. Environ. Chem. Eng. 9 (2021) 105877. https://doi.org/10.1016/j.jece.2021.105877.
[127] A. Nadeali, S. Kalantari, M. Yarmohammadi, M. Omidkhah, A. Ebadi Amooghin, M. Zamani Pedram, CO_2 Separation Properties of a Ternary Mixed-Matrix Membrane Using Ultraselective Synthesized Macrocyclic Organic Compounds, ACS Sustain. Chem. Eng. 8 (2020) 12775–12787. https://doi.org/10.1021/acssuschemeng.0c01895.

[128] S. Miri, M. Omidkhah, A. Ebadi Amooghin, T. Matsuura, Membrane-based gas separation accelerated by quaternary mixed matrix membranes, J. Nat. Gas Sci. Eng. 84 (2020) 103655. https://doi.org/10.1016/j.jngse.2020.103655.
[129] R. He, S. Cong, S. Xu, S. Han, H. Guo, Z. Liang, J. Wang, Y. Zhang, CO2-philic mixed matrix membranes based on low-molecular-weight polyethylene glycol and porous organic polymers, J. Membr. Sci. 624 (2021) 119081. https://doi.org/10.1016/j.memsci.2021.119081.
[130] B. Zhang, C. Yang, Y. Zheng, Y. Wu, C. Song, Q. Liu, Z. Wang, Modification of CO2-selective mixed matrix membranes by a binary composition of poly(ethylene glycol)/NaY zeolite, J. Membr. Sci. 627 (2021) 119239. https://doi.org/10.1016/j.memsci.2021.119239.

List of figures

No color should be used for the figures in print.

List of tables